Article

Cell Host & Microbe

The antagonistic role of an E3 ligase pair in regulating plant NLR-mediated autoimmunity and fungal pathogen resistance

Graphical abstract

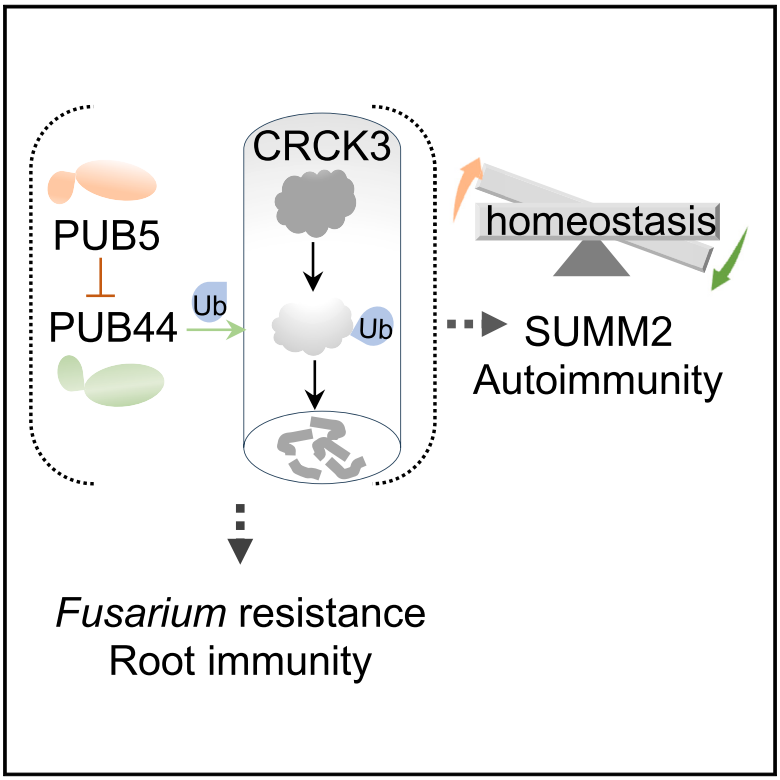

Authors

Jun Liu, Yong Yang, Fausto Andres Ortiz-Morea, ..., Eugenia Russinova, Libo Shan, Ping He

Correspondence

pinghemi@umich.edu

In brief

Two closely related plant U-box E3 ligases, PUB5 and PUB44, antagonistically regulate protein kinase CRCK3 proteostasis in modulating NLR SUMM2-mediated autoimmunity and *Fusarium oxysporum* resistance in *Arabidopsis* and cotton.

Highlights

- The putative plant U-box E3 ligase PUB5 regulates SUMM2-mediated autoimmunity
- PUB5 stabilizes CRCK3, a cytoplasmic kinase involved in SUMM2 activation
- PUB44 monoubiquitylates and degrades CRCK3, which is counteracted by PUB5
- CRCK3 confers resistance to *Fusarium oxysporum* in both *Arabidopsis* and cotton

Liu et al., 2024, Cell Host & Microbe *32*, 1–15
July 10, 2024
https://doi.org/10.1016/j.chom.2024.06.004

CellPress

Cell Host & Microbe

CellPress

Article

The antagonistic role of an E3 ligase pair in regulating plant NLR-mediated autoimmunity and fungal pathogen resistance

Jun Liu,[1,2,6] Yong Yang,[1,6] Fausto Andres Ortiz-Morea,[1,3,4] Yulu Zhou,[3] Derui Liu,[1,5] Yanyan Huang,[1] Jiarui Zheng,[2] Yan Chen,[2] Liang Kong,[1,3] Zunyong Liu,[1,3] Dongdong Ge,[1] Mingli Yong,[1] Wenwei Lin,[1] Eugenia Russinova,[5] Libo Shan,[1,3] and Ping He[1,3,7,*]

[1]Department of Biochemistry & Biophysics, Texas A&M University, College Station, TX 77843, USA
[2]State Key Laboratory of Biocontrol and Guangdong Provincial Key Laboratory of Plant Resources, School of Life Sciences, Sun Yat-Sen University, Guangzhou 510275, China
[3]Department of Molecular, Cellular, & Developmental Biology, University of Michigan, Ann Arbor, MI 48109, USA
[4]Amazonian Research Center Cimaz-Macagual, University of the Amazon, Florencia 180002622, Colombia
[5]Department of Plant Biotechnology & Bioinformatics, Ghent University, and Center for Plant Systems Biology, VIB, Ghent 9052, Belgium
[6]These authors contributed equally
[7]Lead contact
*Correspondence: pinghemi@umich.edu
https://doi.org/10.1016/j.chom.2024.06.004

SUMMARY

Plant immune homeostasis is achieved through a balanced immune activation and suppression, enabling effective defense while averting autoimmunity. In *Arabidopsis*, disrupting a mitogen-activated protein (MAP) kinase cascade triggers nucleotide-binding leucine-rich-repeat (NLR) SUPPRESSOR OF *mkk1/2 2* (SUMM2)-mediated autoimmunity. Through an RNAi screen, we identify PUB5, a putative plant U-box E3 ligase, as a critical regulator of SUMM2-mediated autoimmunity. In contrast to typical E3 ligases, PUB5 stabilizes CRCK3, a calmodulin-binding receptor-like cytoplasmic kinase involved in SUMM2 activation. A closely related E3 ligase, PUB44, functions oppositely with PUB5 to degrade CRCK3 through monoubiquitylation and internalization. Furthermore, CRCK3, highly expressed in roots and conserved across plant species, confers resistance to *Fusarium oxysporum*, a devastating soil-borne fungal pathogen, in both *Arabidopsis* and cotton. These findings demonstrate the antagonistic role of an E3 ligase pair in fine-tuning kinase proteostasis for the regulation of NLR-mediated autoimmunity and highlight the function of autoimmune activators in governing plant root immunity against fungal pathogens.

INTRODUCTION

Plants have developed a highly intricate and sophisticated innate immune system that employs two-tiered immune receptors to effectively safeguard against infections.[1,2] The plasma membrane (PM)-localized pattern recognition receptors (PRRs) recognize microbe-associated molecular patterns (MAMPs) or host-derived danger-associated molecular patterns (DAMPs) to activate pattern-triggered immunity (PTI).[3–5] The intracellular nucleotide-binding leucine-rich-repeat (NLR) proteins directly or indirectly sense pathogen effectors and mediate effector-triggered immunity (ETI).[6]

MAMP perception activates two mitogen-activated protein kinase (MAPK) cascades, MEKK3/5-MKK4/5-MPK3/6 and MEKK1-MKK1/2-MPK4, in *Arabidopsis*.[7–9] Depleting the MEKK1-MKK1/2-MPK4 cascade triggers autoimmunity with *mekk1*, *mkk1 mkk2* (*mkk1/2*), and *mpk4* mutants exhibiting defense gene activation, cell death, and seedling lethality.[10–14] Genetic screens for suppressors of the *mkk1/2* lethality have revealed the NLR protein SUPPRESSOR OF *mkk1/2 2* (SUMM2), the MAPK kinase kinase MEKK2, and the calmodulin-binding receptor-like cytoplasmic kinase (RLCK) CRCK3 as essential regulators of the *mekk1-mkk1/2-mpk4* autoimmunity.[15–17] MEKK2 and CRCK3 were also revealed as suppressors of *mekk1* lethality (LETs) using an RNAi-based screen toward transfer DNA (T-DNA) insertional mutant collections.[18] LET1 encodes a PM-resident malectin-like receptor kinase (RK) (MLR) that complexes with MEKK2 and SUMM2.[19] MEKK2 scaffolds LET1 and SUMM2 for protein stability regulation by counteracting the F-box protein CPR1-mediated SUMM2 ubiquitylation and degradation.[19] MEKK2 likely plays a structural role linking PM-resident RKs and intracellular NLR rather than functioning as an authentic kinase in regulating *mekk1-mkk1/2-mpk4* autoimmunity.[18,20] This further corroborates an early observation of the importance of precise regulation of the transcript and protein abundance of MEKK2, overexpression of which induces SUMM2-dependent cell death.[16,21]

LET2, another MLR, functions together with LET1 and LORELEI-like glycosylphosphatidylinositol (GPI)-anchored protein 1 (LLG1),

Please cite this article in press as: Liu et al., The antagonistic role of an E3 ligase pair in regulating plant NLR-mediated autoimmunity and fungal pathogen resistance, Cell Host & Microbe (2024), https://doi.org/10.1016/j.chom.2024.06.004

forming a trimeric complex regulating SUMM2 activation.[22] LET2 phosphorylates LET1, and their kinase activities are vital for their functions in *mekk1-mkk1/2-mpk4* autoimmunity.[19,22] LET2 was also identified in a suppressor screen for the *mkk1/2/ndr1* lethality and interacts with and phosphorylates CRCK3.[23] The CRCK3 protein level is critical in SUMM2-mediated autoimmunity.[18] How the CRCK3 proteostasis is regulated remains elusive.

Suppressor screens for dwarfism resulting from the overexpression of the MEKK1 N-terminal domain (SMN) have identified NLR RPS6 and the DEAD-box RNA helicase SMN2/HEN2, which forms part of the nuclear RNA exosome necessary for the accumulation of *RPS6* transcripts.[24,25] Interestingly, the *rps6* mutant partially and conditionally suppressed *mekk1* and *mpk4* autoimmunity in the L*er* ecotype at a high temperature (26°C).[24] Nevertheless, these observations imply the potential involvement of additional NLRs safeguarded by the MEKK1-MKK1/2-MPK4 cascade to maintain immune homeostasis.

Here, we report that an RNAi screen for suppressors of the *mekk1* lethality reveals PUB5, a putative plant U-box (PUB) E3 ligase, as an important regulator of *mekk1-mkk1/2-mpk4* autoimmunity. Epistasis analysis depicts that PUB5 functions genetically downstream of MEKK2 and upstream of SUMM2. Surprisingly, similar to wide-type (WT) PUB5, its E2-binding site mutants could complement the *pub5* defect in triggering *mekk1* cell death. Additionally, PUB5 stabilizes CRCK3, which was identified as an interactor of PUB5 from a yeast two-hybrid screen. A proteomics approach identified PUB44, a closely related E3 ligase of PUB5, as an interactor of CRCK3. PUB44 monoubiquitylates CRCK3, leading to CRCK3 internalization and degradation. PUB5 counteracts PUB44-mediated CRCK3 monoubiquitylation and internalization, thereby stabilizing CRCK3. Thus, the CRCK3 proteostasis is inversely regulated by PUB5 and PUB44 in maintaining a balanced immune response. CRCK3 and PUB5 are conserved across various plant species and highly expressed in roots, with a crucial role in preventing the invasion of the soil-borne pathogen *Fusarium oxysporum* into vascular tissues of both *Arabidopsis* and cotton.

RESULTS

The *pub5* mutants suppress the *mekk1-mkk1/2-mpk4* autoimmunity

To gain insight into the immune homeostasis regulation, we carried out genetic screens for suppressors of virus-induced gene silencing (VIGS) of *MEKK1*-triggered cell death toward *Arabidopsis* T-DNA mutant collections. Multiple suppressors of *mekk1* lethality (*letum* or *let*) mutants were isolated.[18] The *let3* mutant suppressed plant dwarfism and leaf chlorosis, cell death detected by trypan blue staining, elevated H_2O_2 production detected by 3, 3′-diaminobenzidine (DAB) staining, and enhanced *PR1* and *PR2* expression triggered by silencing *MEKK1* (Figures 1A–1C). Notably, the *let3* mutant did not affect the growth defects and cell death caused by RNAi-*BRI1-ASSOCIATED RECEPTOR KINASE 1* (*BAK1*) and *SOMATIC EMBRYOGENESIS RECEPTOR-LIKE KINASE 4* (*SERK4*)[26] (Figure 1A), indicating a specific role of *LET3* in *MEKK1*-mediated cell death.

Based on the annotation in *Arabidopsis* information resource (TAIR), the *let3* mutant (*salk_144599c*) carries a T-DNA insertion in the second exon of *AT3G28040*, encoding an uncharacterized RK (Figure S1A). We obtained two additional T-DNA insertional lines (*salk_053567* and *salk_093475*) for *AT3G28040* (Figures S1A and S1B). However, these two lines did not suppress the cell death induced by silencing *MEKK1* (Figure S1C), suggesting that *AT3G28040* may not be the causal gene of *LET3* in *MEKK1*-mediated cell death.

We then performed positional cloning to identify the causative mutation responsible for the *mekk1* cell death suppression in *let3*. We first generated the *let3/mekk1* double mutant, which substantially suppressed *mekk1* cell death (see below), and then crossed *let3/mekk1* (in the Col-0 background) with the L*er*-0 ecotype to generate an F_2 mapping population. Linkage analysis using 205 plants with *let3/mekk1*-like phenotypes indicated that the *let3* mutation was between markers *M4E13* and *F20D10* on chromosome 4 (Figure S1D). Whole-genome resequencing of *let3* revealed an 818-bp deletion in *AT4G36550*. *AT4G36550* encodes the plant U-box protein PUB5 with a U-box N-terminal domain (UND), a U-box domain, and three repeats of the C-terminal armadillo (ARM) motif (Figure 1D). The deletion in *let3* was confirmed by PCR and Sanger sequencing (Figure S1E). The *let3* mutant, which was renamed *pub5-1*, produced a truncated protein with a partial UND (Figure 1D).

We isolated another allele, *gabi_003b11*, named *pub5-2*, which harbors a T-DNA insertion in the 3′ UTR of *PUB5* and shows the reduced accumulation of *PUB5* transcripts (Figures S1F and S1G). Similar to *pub5-1*, *pub5-2* suppressed cell death triggered by RNAi-*MEKK1* (Figure S1H). Additionally, we expressed the *PUB5* genomic DNA tagged with *GFP* at its C terminus under its native promoter in *pub5-1* (*pPUB5::gPUB5-GFP/pub5-1*). Three independent transgenic lines restored plant growth defects caused by RNAi-*MEKK1* (Figure 1E), confirming that the suppression of RNAi-*MEKK1* cell death is due to the mutation in *PUB5*.

The *pub5-1/mekk1* double mutant suppressed plant dwarfism, cell death, elevated H_2O_2 accumulation, and expression of *PR1* and *PR2* in *mekk1* (Figures 1F and 1G). We further generated the *pub5-1/mkk1/2* triple mutant and *pub5-1/mpk4* double mutant. Plant dwarfism, cell death, elevated H_2O_2 accumulation, and expression of *PR1* and *PR2* in *mkk1/2* and *mpk4* mutants were largely suppressed in *pub5-1/mkk1/2* and *pub5-1/mpk4* (Figures 1F and 1G). Together, these results indicate that PUB5 functions downstream of the MEKK1-MKK1/2-MPK4 kinase cascade in regulating autoimmunity.

PUB5 functions genetically downstream of MEKK2 and upstream of SUMM2

Overexpression of *MEKK2* triggers SUMM2-dependent cell death.[15,21] To analyze whether *PUB5* is required for autoimmune responses induced by overexpression of *MEKK2*, we overexpressed *MEKK2-HA* under the *35S* promoter in WT and *pub5-1*. Plant dwarfism, cell death, elevated H_2O_2 accumulation, and expression of *PR1* and *PR2* observed in *p35S::MEKK2-HA*/WT transgenic plants were substantially reduced in *p35S::MEKK2-HA/pub5-1* transgenic plants (Figures 1H and S1I). MEKK2-HA expression levels in WT and *pub5-1* were similar (Figure S1J). These data indicate that *MEKK2* overexpression-triggered autoimmunity requires *PUB5*.

Please cite this article in press as: Liu et al., The antagonistic role of an E3 ligase pair in regulating plant NLR-mediated autoimmunity and fungal pathogen resistance, Cell Host & Microbe (2024), https://doi.org/10.1016/j.chom.2024.06.004

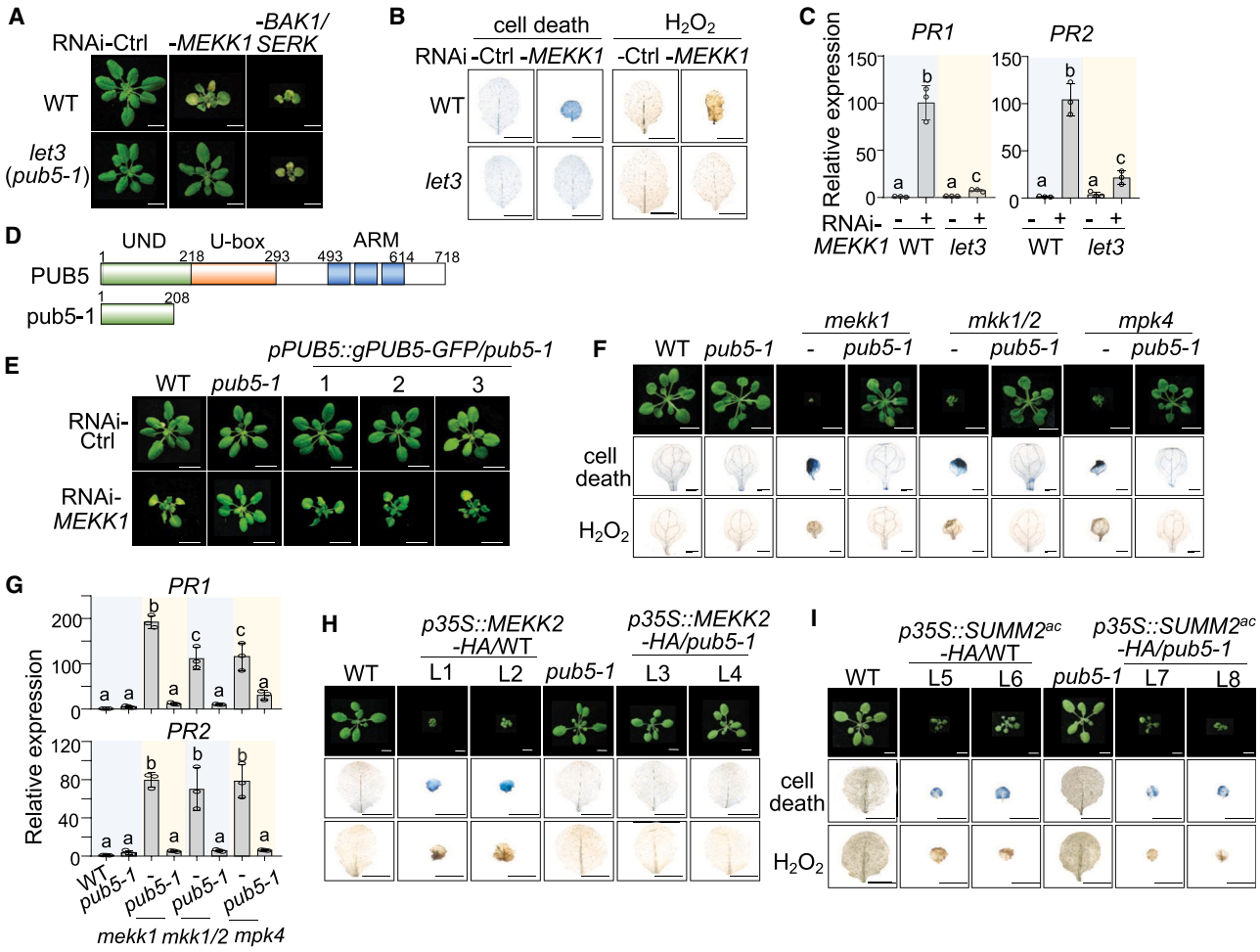

Figure 1. The *pub5* mutants suppress *mekk1-mkk1/2-mpk4* autoimmunity

(A) The *let3* (*pub5-1*) mutant suppresses growth defects triggered by RNAi-*MEKK1*. Plants are shown 3 weeks after VIGS. Scale bars, 1 cm.

(B) The *let3* mutant suppresses cell death (left) and H_2O_2 accumulation (right) triggered by RNAi-*MEKK1*. Scale bars, 0.5 cm.

(C) The *let3* mutant suppresses *PR1* and *PR2* expression triggered by RNAi-*MEKK1*. Data are shown as mean ± SD ($n = 3$).

(D) The predicted protein domains of WT PUB5 and pub5-1. Domains with amino acid positions labeled on the top were identified using the Uniprot (https://www.uniprot.org/) database.

(E) Complementation of *pub5-1* with *pPUB5::gPUB5-GFP* restores growth defects induced by RNAi-*MEKK1*. Three independent complementation lines are shown. Scale bars, 1 cm.

(F) The *pub5-1* mutant suppresses growth defects, cell death, and H_2O_2 accumulation of *mekk1*, *mkk1/2*, and *mpk4* mutants. 3-week-old seedlings are shown (upper, scale bars, 1 cm). Cotyledons were stained with trypan blue for cell death (middle) and DAB (bottom) for H_2O_2 (scale bars, 1 mm).

(G) The *pub5-1* mutant suppresses the elevated *PR1* and *PR2* expression of *mekk1*, *mkk1/2*, and *mpk4* mutants. Data are shown as mean ± SD ($n = 3$).

(H and I) The *pub5-1* mutant suppresses *MEKK2* (H), but not *SUMM2*^{ac} (I), overexpression-induced plant growth defects, cell death, and H_2O_2 accumulation. Scale bars: 1 cm (top) and 0.5 cm (middle and bottom).

Experiments were repeated three times with similar results. Different letters in (C) and (G) indicate a statistically significant difference according to a one-way ANOVA followed by the Tukey test ($p < 0.05$).

See also Figure S1.

The expression of constitutively active SUMM2 (SUMM2^{ac}) causes cell death in tobacco and *Arabidopsis*.[15,19] We overexpressed *SUMM2*^{ac}*-HA* under the *35S* promoter in WT and *pub5-1*. Transgenic plants in WT and *pub5-1* with comparable SUMM2^{ac}-HA expression exhibited similar levels of autoimmune phenotypes, including dwarfism, cell death, elevated H_2O_2 production, and overaccumulation of *PR1* and *PR2* (Figures 1I, S1K, and S1L), indicating that SUMM2^{ac}-induced cell death does not require PUB5. Together, our epistasis analysis suggests that PUB5 acts genetically between MEKK2 and SUMM2.

PUB5 interacts with CRCK3

To understand how PUB5 regulates SUMM2-mediated autoimmunity, we performed a yeast two-hybrid screen using PUB5 as the bait against an *Arabidopsis* cDNA library to identify PUB5-interacting proteins. Among 12 strong interactors (Figures 2A and S2A), CRCK3, also known as SUMM3, functions genetically between MEKK2 and SUMM2 in the *mekk1-mkk1/2-mpk4* cell death pathway.[17,18] To confirm the interaction of PUB5 with CRCK3, we purified the glutathione S-transferase (GST)-tagged cytosolic domain (CD, 225th to 510th residues) of

Please cite this article in press as: Liu et al., The antagonistic role of an E3 ligase pair in regulating plant NLR-mediated autoimmunity and fungal pathogen resistance, Cell Host & Microbe (2024), https://doi.org/10.1016/j.chom.2024.06.004

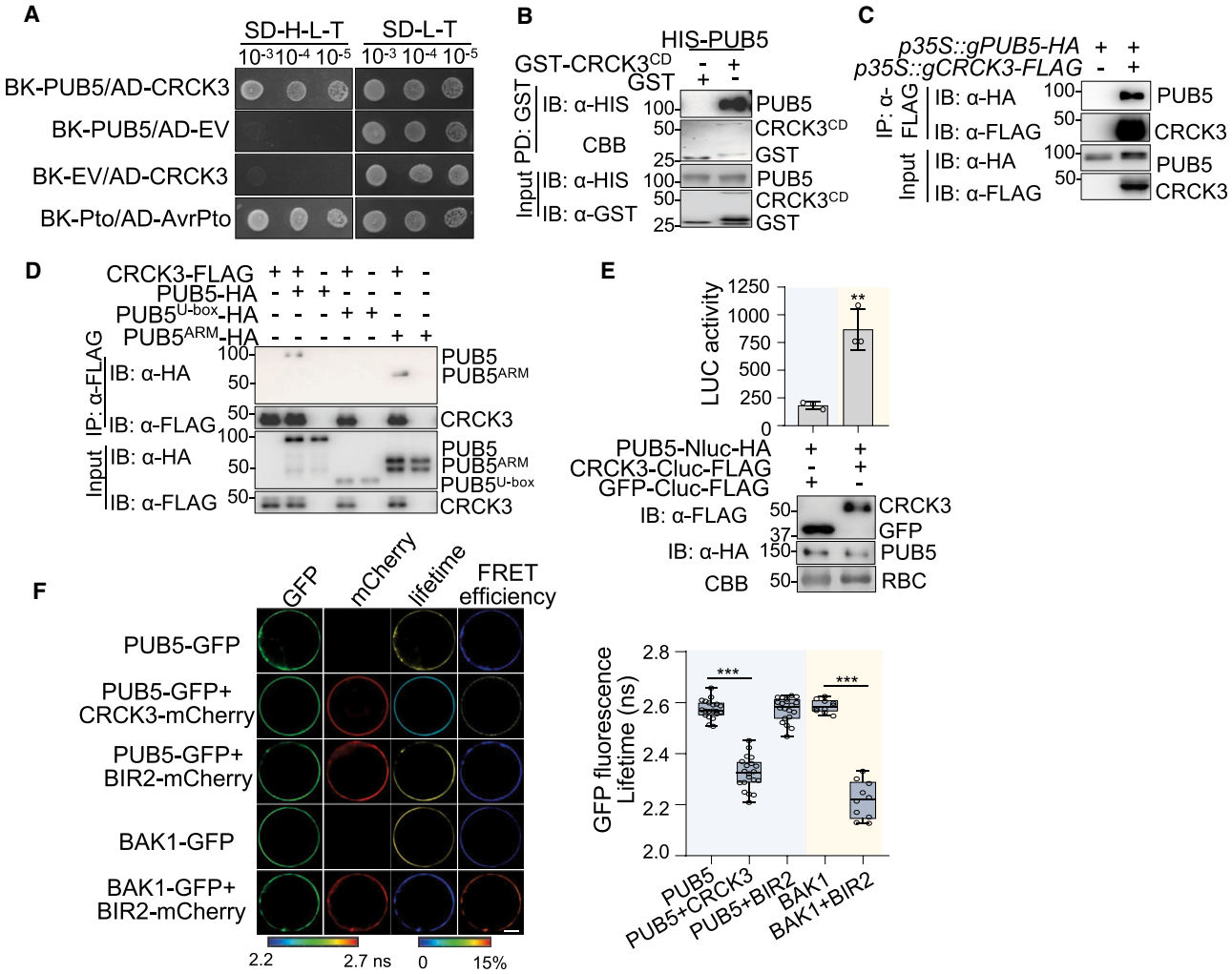

Figure 2. PUB5 interacts with CRCK3

(A) CRCK3 interacts with PUB5 in yeast. Yeast carrying BK-PUB5 and AD-CRCK3 was grown on a synthetic defined (SD) medium without histidine, leucine, and tryptophan (SD-H-L-T) with 3-AT. EV indicates empty vectors. Pto and AvrPto interaction was used as a positive control.

(B) PUB5 interacts with CRCK3^{CD} in an *in vitro* pull-down (PD) assay. GST or GST-CRCK3^{CD} glutathione-agarose was incubated with HIS-PUB5. Washed beads were pelleted for immunoblotting or stained with Coomassie brilliant blue (CBB) (top two). Input proteins were immunoblotted before the pull-down (bottom two). Molecular weight with kDa as the unit was labeled on the left of all immunoblots in this study.

(C) PUB5 associates with CRCK3 by a co-immunoprecipitation (coIP) assay. Total proteins from transgenic plants were isolated for the assay (top two), with input controls shown (bottom two).

(D) PUB5 ARM domain associates with CRCK3 in protoplasts.

(E) CRCK3 associates with PUB5 in a split-luciferase assay in protoplasts. Protein expression is shown on the bottom with Rubisco (RBC) stained by CBB for protein loading. Data are shown as mean ± SD (n = 3).

(F) CRCK3 associates with PUB5 in a FRET-FLIM assay in protoplasts. Localization of GFP- and mCherry-tagged proteins is shown in the first (green) and second column (red), respectively. The lifetime (τ) distribution (third column) and FRET efficiency (fourth column) are presented as pseudo-color images according to the scale (left). The GFP mean fluorescence lifetime (τ) values are shown as box plots as defined in the STAR Methods (n = 20 for the first three columns and 10 for the last two columns, right). BAK1-GFP and BIR2-mCherry were included as a control. Scale bars, 10 μm.

Experiments were repeated three times with similar results. Asterisks in (E) and (F) represent significant differences using a two-sided, two-tailed Student's t test (** $p < 0.01$, *** $p < 0.001$).

See also Figure S2.

CRCK3 (GST-CRCK3^{CD}) and 6×HIS-tagged PUB5 (HIS-PUB5) from *E. coli*. and performed an *in vitro* pull-down assay. GST-CRCK3^{CD}, but not GST alone, pulled down HIS-PUB5, indicating a direct interaction between PUB5 and CRCK3 (Figure 2B). Co-immunoprecipitation (coIP) assays using transgenic plants carrying PUB5-HA and CRCK3-FLAG under the *35S* promoter confirmed that PUB5 associated with CRCK3 *in planta* (Figure 2C). The association of PUB5 and CRCK3 was also detected by a coIP assay when PUB5 and CRCK3 were expressed in protoplasts (Figure S2B). The ARM domain, but not the U-box, of PUB5 mediated the association with CRCK3 (Figures 2D and S2C). This is further corroborated by the CRCK3-PUB5 complex

Please cite this article in press as: Liu et al., The antagonistic role of an E3 ligase pair in regulating plant NLR-mediated autoimmunity and fungal pathogen resistance, Cell Host & Microbe (2024), https://doi.org/10.1016/j.chom.2024.06.004

structure predicted by the ColabFold platform using the AlphaFold2 source code,[27] in which CRCK3 complexes with PUB5 through three interfaces (IFs), namely IF1, IF2, and IF3, located at PUB5 ARM domain (Figures S2D and S2E). Mutation of IF1 in PUB5 (arginine 576 [R576], cysteine 612 [C612], glutamine 614 [Q614], and R653 to alanine [A]) compromised its association with CRCK3, and further mutations of IF2 (leucine 320 [L320] and tyrosine 321 [Y321]) and IF3 (Y338 and isoleucine 340 [I340]) in PUB5 IF1 mutant substantially reduced its association with CRCK3 (Figure S2E), indicating that these IFs located at PUB5 are essential for its binding to CRCK3. Additionally, co-expression of CRCK3 fused with the C-terminal half of luciferase (CRCK3-Cluc) and PUB5 fused with the N-terminal half of luciferase (PUB5-Nluc) reconstituted luciferase signals compared with GFP-Cluc controls (Figure 2E). Moreover, Förster resonance energy transfer (FRET)-fluorescence lifetime imaging (FLIM) experiments revealed that PUB5-GFP was in the close vicinity of CRCK3-mCherry on the PM (Figure 2F). Taken together, PUB5 directly interacts with CRCK3 via the ARM domain.

PUB5 stabilizes CRCK3 proteins in aggravating *mekk1* autoimmunity

We observed that the loss of RNAi-*MEKK1* autoimmunity in *pub5-1* could be restored by overexpression of *p35S::gCRCK3-GFP* (Figure 3A), suggesting that the incapacity to induce *mekk1* autoimmunity in *pub5* might be attributed to decreased protein levels of CRCK3. Indeed, CRCK3-GFP protein levels in multiple transgenic lines in *pub5-1* were lower than in WT (Figure 3B). Conversely, co-expression of PUB5-HA led to increased protein levels of CRCK3-GFP, but not GFP, in *Nicotiana benthamiana* (Figure 3C). Furthermore, expression of *p35S::gPUB5-HA* in *pCRCK3::gCRCK3-GFP/pub5-1* or *p35S::gCRCK3-GFP/pub5-1* transgenic plants increased CRCK3-GFP protein levels (Figures 3D and S3A). Moreover, the protein abundance of CRCK3-GFP and PUB5-HA was positively correlated (Figure S3A). CRCK3 undergoes proteasome-dependent protein degradation.[18] PUB5 likely stabilizes CRCK3 proteins by blocking their degradation. Consistently, the fluorescent signal intensity on the PM of *p35S::gCRCK3-GFP* transgenic plants in *pub5-1* was substantially lower than in WT (Figure 3E). Notably, overexpression of *PUB5* did not affect protein levels of other components involved in *mekk1* cell death regulation, including LET1, MEKK2, and SUMM2, when transiently expressed in *N. benthamiana* (Figures S3B–S3D). The data point to a crucial role of PUB5 in the specific regulation of CRCK3 stability in triggering *mekk1* autoimmunity.

Since *pub5* mutants suppress *mekk1* cell death (Figure 1F), we examined whether overexpression of *PUB5* could promote *mekk1* cell death by transforming *p35S::gPUB5-FLAG* into *mekk1* heterozygous plants. Multiple *p35S::gPUB5-FLAG/mekk1* lines displayed enhanced dwarfism compared with *mekk1* (Figure 3F), indicating that PUB5 augments *mekk1* cell death. Notably, CRCK3 protein levels are important in *mekk1* cell death.[18] Consistently, *p35S::gCRCK3-GFP*/WT transgenic plants exhibited enhanced cell death upon silencing *MEKK1* compared with WT plants (Figure S3E). Thus, it is conceivable that PUB5 aggravates *mekk1* autoimmunity by increasing CRCK3 protein levels.

PUB E3 ubiquitin (UBQ) ligases control the stability of substrate proteins and typically decrease the abundance of their target proteins.[28] It is unexpected that PUB5 interacts with but promotes CRCK3 protein levels. In addition, PUB5 did not display any measurable autoubiquitylation activities with different E2 enzymes *in vitro* (Figures S3F and S3G). PUB5 contains the conserved E2-binding motif in the U-box domain, and the corresponding residues of cysteine at position 225 (C^{225}) and tryptophan at position 252 (W252) in PUB10, PUB12, and PUB13 are essential for their E3 ligase activities (Figure S3H).[29,30] Surprisingly, transgenic plants of *p35S::gPUB5*^{C225A}*-GFP* or *p35S::gPUB5*^{W252A}*-GFP* could complement *pub5* in triggering RNAi-*MEKK1* autoimmunity (Figure 3G). In addition, like PUB5, PUB5^{C225A}, or PUB5^{W252A} increased CRCK3-HA protein abundance when co-expressing in *N. benthamiana* (Figure S3I). Furthermore, the PUB5 ARM domain, but not the U-box domain, stabilized CRCK3 (Figure S3J). The PUB5 mutant, IF1,2,3, with mutations in three IFs with CRCK3, reduced the ability to stabilize CRCK3 (Figure S3K), suggesting that PUB5 binding to CRCK3 is essential for stabilizing CRCK3. Together, the data highlight that PUB5 may not function as a typical E3 ligase to ubiquitylate and degrade substrate proteins.

PUB44 interacts with CRCK3 in regulating SUMM2-mediated autoimmunity

We further performed IP-based proteomics by liquid chromatography-tandem mass spectrometry (LC-MS/MS) analysis to identify CRCK3-associated proteins. Enriched coverages of CRCK3, as well as several known CRCK3-interacting proteins, such as LET2, LET1, and PUB5, indicate the efficiency of IP and MS analysis (Figure S3L). Interestingly, PUB44, also named senescence-associated E3 ubiquitin ligase 1 (SAUL1) and belonging to the same phylogenetic subclade as PUB5, is among CRCK3-associated proteins (Figures S3L and S3M). When co-expressing in protoplasts or transgenic plants (*p35S::gPUB44-HA/p35S::gCRCK3-FLAG*), CRCK3-FLAG immunoprecipitated PUB44-HA (Figures 4A and S4A). The association of PUB44 and CRCK3 was also detected by split-luciferase complementation assays, as co-expression of CRCK3-Cluc and PUB44-Nluc reconstituted luciferase activities compared with controls (Figure S4B). FRET-FLIM assays revealed that PUB44-GFP was in close proximity to CRCK3-mCherry on the PM (Figure 4B). In addition, GST-CRCK3^{CD} pulled down HIS-PUB44 *in vitro* (Figure 4C). These results indicate that PUB44 directly interacts with CRCK3.

Depletion of PUB44 leads to the initiation of NLR suppressors of *chs1-2*, 3 (SOC3)-dependent autoimmunity.[31–33] Importantly, the seedling lethality of *pub44* was partially alleviated in the *pub44/summ3-17* and *pub44/summ2-8* double mutants (Figures 4D, S4C, and S4D), underscoring that depletion of PUB44 activates the CRCK3-SUMM2 pathway. Interestingly, the *soc3-21* mutant does not appear to affect RNAi-*MEKK1*-triggered autoimmunity (Figure S4E), suggesting that SOC3 and SUMM2 function independently in triggering autoimmunity.

PUB44 reduces the CRCK3 protein abundance

We transformed *pCRCK3::gCRCK3-GFP* into the *pub44* heterozygous mutants. CRCK3-GFP expression levels were elevated in the *pub44* homozygous mutant compared with those in WT (Figure 4E). The fluorescent signals in the leaves and roots of *pCRCK3::gCRCK3-GFP* transgenic plants were also substantially increased in *pub44* compared with those in WT (Figures 4F and

Please cite this article in press as: Liu et al., The antagonistic role of an E3 ligase pair in regulating plant NLR-mediated autoimmunity and fungal pathogen resistance, Cell Host & Microbe (2024), https://doi.org/10.1016/j.chom.2024.06.004

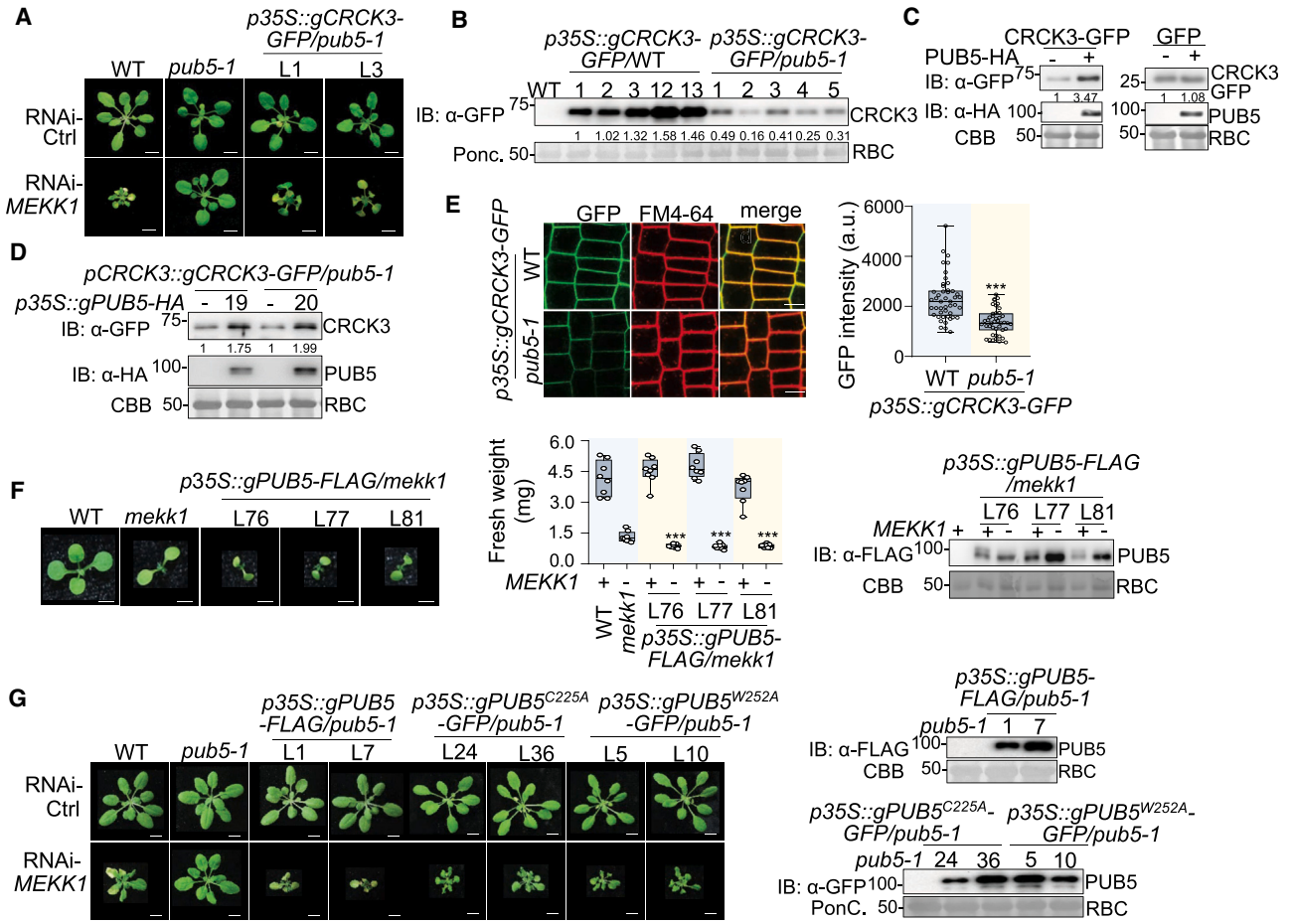

Figure 3. PUB5 stabilizes CRCK3 in promoting *mekk1* cell death

(A) CRCK3 overexpression restores silencing *MEKK1*-triggered cell death in *pub5-1*. Scale bars, 1 cm.

(B) CRCK3-GFP protein levels are reduced in *pub5-1* compared with WT. CRCK3-GFP protein expression in multiple transgenic lines of *p35S::gCRCK3-GFP* in WT or *pub5-1* is shown (top). Ponceau S (Ponc.) staining of RBC indicates protein loading (bottom).

(C) PUB5 enhances CRCK3 protein abundance. CRCK3-GFP or GFP was co-expressed with PUB5-HA or vector (−) in *N. benthamiana*.

(D) PUB5 overexpression in *pCRCK3::gCRCK3-GFP/pub5-1* increases CRCK3 protein levels.

(E) CRCK3-GFP expression in *pub5-1* is reduced compared with WT. Root tips of 4-day-old transgenic plants were imaged by confocal microscopy. FM4-64 staining indicates the PM. Scale bars: 10 μm (left). CRCK3-GFP intensity of transgenic plants in WT (n = 46) or *pub5-1* (n = 43) is shown as box plots (right).

(F) PUB5 overexpression aggravates *mekk1* seedling lethality. Three independent 2-week-old transgenic lines are shown. Scale bars: 0.1 cm (left). Quantification of fresh weight is shown as box plots (n = 8) (middle). "−" indicates *mekk1* homozygous, and "+" indicates *MEKK1* homozygous plants. PUB5 protein expression is shown (right).

(G) Complementation of PUB5^{C225A} and PUB5^{W252A} restores RNAi-*MEKK1*-induced growth defects in *pub5-1*. Scale bars, 1 cm. PUB5 protein expression is shown (right).

Experiments were repeated three times with similar results. Numbers under immunoblots (B–D) indicate the relative densitometry of corresponding bands after normalizing to the control. Asterisks in (E) and (F) indicate statistical significance using a two-sided, two-tailed Student's t test (*** $p < 0.001$).

See also Figure S3.

S4F). To eliminate the effects of the transcriptional regulation of *CRCK3, CRCK3-GFP* under the *35S* promotor (*p35S::gCRCK3-GFP*) was transformed into the *pub44* heterozygous mutant. The fluorescence signals of *p35S::gCRCK3-GFP* transgenic plants were also elevated in *pub44* compared with WT (Figure 4G). Consistently, silencing *PUB44* by VIGS in *p35S::gCRCK3-GFP*/WT transgenic plants led to the increased abundance of CRCK3 proteins in multiple lines (Figure S4G). Conversely, overexpression of PUB44-HA, but not PUB13-HA, in *p35S::gCRCK3-GFP* transgenic plants led to the reduced protein abundance and fluorescent signals of CRCK3-GFP (Figures 4H, 4I, S4H, and S4I). The data indicate that PUB44 reduces CRCK3 protein abundance and negatively regulates CRCK3 stability.

PUB44 mediates CRCK3 monoubiquitylation

We then examined whether PUB44 possesses E3 ligase activities and ubiquitylates CRCK3, thereby regulating CRCK3 proteostasis. An *in vitro* ubiquitylation assay showed that HIS-PUB44, but not HIS-PUB44^{C29A}, which carries the mutation in the conserved catalytic cysteine residue at position 29 to alanine (C29A),[33] was autoubiquitylated (Figures S4J and S4K). The observed ubiquitylation appears to be in the form of

Please cite this article in press as: Liu et al., The antagonistic role of an E3 ligase pair in regulating plant NLR-mediated autoimmunity and fungal pathogen resistance, Cell Host & Microbe (2024), https://doi.org/10.1016/j.chom.2024.06.004

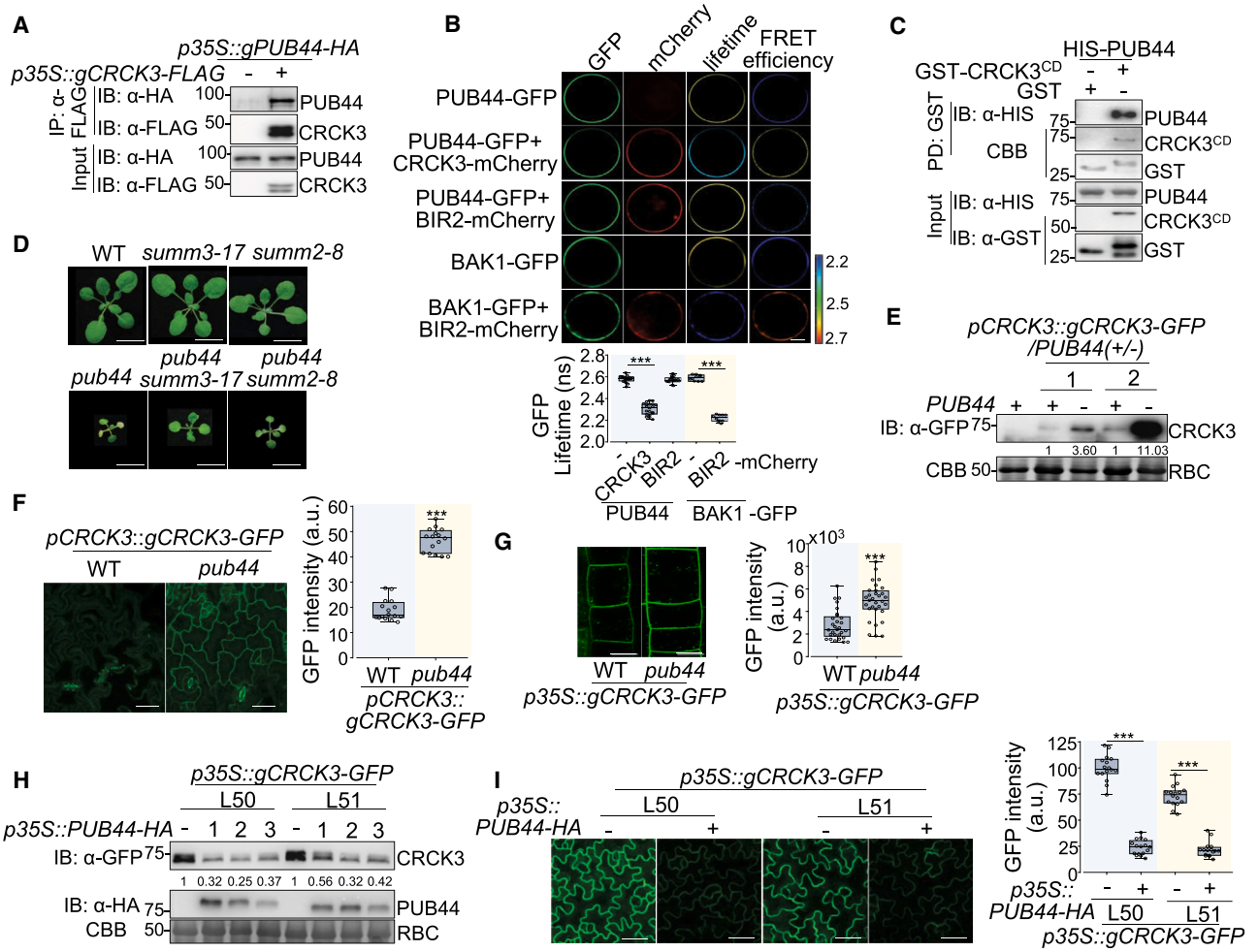

Figure 4. PUB44 reduces CRCK3 protein levels

(A) PUB44 associates with CRCK3 in transgenic plants by a coIP assay.

(B) PUB44 associates with CRCK3 in a FRET-FLIM assay. Data are shown as box plots (n = 20 for the first three columns and 10 for the last two columns). Scale bars, 10 μm.

(C) PUB44 interacts with CRCK3^{CD} in an *in vitro* pull-down assay.

(D) The *crck3* (*summ3-17*) and *summ2-8* mutants alleviate the pub*44* cell death. 3-week-old soil-grown plants are shown. Scale bars, 1 cm.

(E and F) CRCK3 protein expression is enhanced in *pub44* compared with WT. CRCK3-GFP protein expression in WT (+) and *pub44* (–) transgenic lines was detected by immunoblotting (E) and confocal microscopy (F, left, scale bars, 10 μm). Quantification of CRCK3-GFP intensity is shown as box plots (n = 16) (F, right).

(G) The *pub44* mutant accumulates more CRCK3 proteins than WT. Root tips of 5-day-old transgenic plants were imaged by confocal microscopy with 50 μM cycloheximide (CHX) treatment for 2 h. Scale bars: 10 μm (left). Quantification of CRCK3-GFP intensity in WT (n = 29) and *pub44* (n = 31) is shown as box plots (right).

(H and I) PUB44 overexpression reduces CRCK3 protein levels. *p35S::PUB44-HA* was expressed in two independent *p35S::gCRCK3-GFP*/WT transgenic lines. Proteins were detected by immunoblotting (H) and confocal microscopy (I, left). Quantification of CRCK3-GFP intensity is shown as box plots (n = 16) (I, right). Experiments were repeated three times with similar results. Asterisks in (B), (F), (G), and (I) indicate statistical significance using a two-sided, two-tailed Student's t test (*** $p < 0.001$). Numbers under immunoblots in (E) and (H) indicate relative densitometry of corresponding bands after normalizing to the control.

See also Figures S3 and S4.

monoubiquitylation, as evidenced by a discrete band on the immunoblot showing an increase in molecular weight of approximately 8 kDa (Figure S4K). In addition, PUB44 exhibited autoubiquitylation activities in the presence of UBQ, as well as the UBQ^{k0} mutant, which bears mutations in all lysine (K) residues to R and no longer extends the UBQ chain growth (Figures 5A and S4L). Significantly, the *in vitro* ubiquitylation assay showed that HIS-PUB44 monoubiquitylated GST-CRCK3^{CD} in the presence of UBQ or UBQ^{k0} (Figures 5B and S4M). The ubiquitylated band of GST-CRCK3^{CD} by HIS-PUB44 was also detected by an α-UBQ antibody (Figure S4N). Furthermore, GST-tagged USP2-cc, a deubiquitylating enzyme from mouse,[34] removed HIS-PUB44-mediated the shifted band of GST-CRCK3^{CD} (Figure S4O). The data support that CRCK3 is monoubiquitylated by PUB44 *in vitro*. LC-MS/MS analysis identified seven K residues in CRCK3 that were ubiquitylated by PUB44 *in vitro*

Please cite this article in press as: Liu et al., The antagonistic role of an E3 ligase pair in regulating plant NLR-mediated autoimmunity and fungal pathogen resistance, Cell Host & Microbe (2024), https://doi.org/10.1016/j.chom.2024.06.004

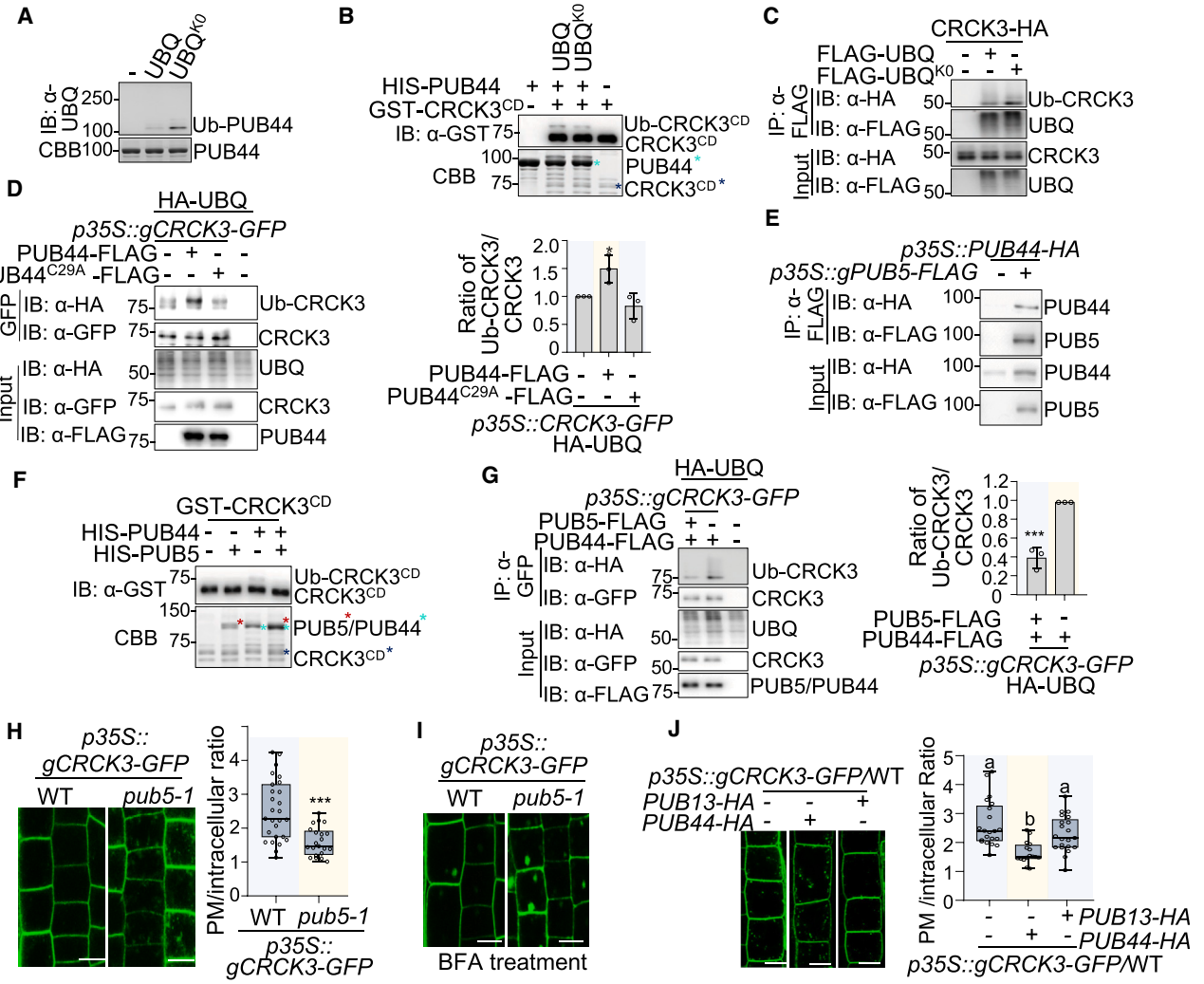

Figure 5. PUB44 and PUB5 oppositely regulate CRCK3 monoubiquitylation

(A) PUB44 possesses monoubiquitylation activity *in vitro*. Ubiquitylation was detected by an α-UBQ antibody (top). CBB staining indicates protein loading (bottom).

(B) PUB44 monoubiquitylates CRCK3 *in vitro*. Ubiquitylated GST-CRCK3^{CD} was detected as a mobility shift by an α-GST antibody (top).

(C) Monoubiquitylation of CRCK3 *in planta*. CRCK3-HA was co-expressed with FLAG-UBQ, FLAG-UBQ^{k0}, or vector (−) in protoplasts for the immunoprecipitation assay.

(D) PUB44 enhances CRCK3 monoubiquitylation. HA-UBQ was co-expressed with PUB44-FLAG or PUB44^{C29A}-FLAG in protoplasts from *p35S::gCRCK3-GFP* transgenic plants or control vectors in WT protoplasts (−). Total proteins were used for the immunoprecipitation assay and immunoblotting (left). Quantification of ubiquitylated CRCK3 normalized to the immunoprecipitated CRCK3 is shown as mean ± SD (n = 3, right).

(E) PUB44 associates with PUB5 in transgenic plants in the coIP assay.

(F) PUB5 suppresses PUB44-mediated CRCK3 monoubiquitylation *in vitro*.

(G) PUB5 suppresses PUB44-mediated CRCK3 monoubiquitylation *in vivo*. The *in vivo* ubiquitylation assay and quantification (n = 3) were performed as in (D).

(H) The CRCK3 internalization is enhanced in *pub5-1*. Roots of 5-day-old *p35S::gCRCK3-GFP* transgenic plants in WT (3% of laser power) or *pub5-1* (15% of laser power) were imaged by a confocal microscope after 50 μM CHX treatment for 2 h (left). Quantification of the ratio of CRCK3-GFP fluorescence intensity between the PM and intracellular space in WT (n = 27) or *pub5-1* (n = 21) is shown as box plots (right). Scale bars, 10 μm.

(I) CRCK3-GFP BFA bodies are increased in *pub5-1*. Epidermal cells from root meristems were pretreated with 50 μM CHX for 1.5 h, then 50 μM CHX and 50 μM brefeldin A (BFA) for 30 min before imaging by a confocal microscope. Scale bars, 10 μm.

(J) PUB44, not PUB13, enhances CRCK3 internalization. *p35S::gCRCK3-GFP* was co-expressed with *p35S::PUB44-HA* or *p35S::PUB13-HA* in transgenic plants. Data are shown as box plots (n = 21 for *p35S::gCRCK3-GFP* and *p35S::gCRCK3-GFP/p35S::PUB13-HA*, and 16 for *p35S::gCRCK3-GFP/p35S::PUB44-HA*). Different letters indicate statistically significant differences according to one-way ANOVA followed by the Tukey test ($p < 0.05$). Scale bars, 10 μm.

Experiments were repeated three times with similar results. Asterisks in (D), (G), and (H) indicate a statistical significance using a two-sided, two-tailed Student's t test (* $p < 0.05$, *** $p < 0.001$).

See also Figures S4 and S5.

Please cite this article in press as: Liu et al., The antagonistic role of an E3 ligase pair in regulating plant NLR-mediated autoimmunity and fungal pathogen resistance, Cell Host & Microbe (2024), https://doi.org/10.1016/j.chom.2024.06.004

(Figures S4P and S4Q). Importantly, mutation of all seven K residues to R in CRCK3, CRCK3^{7KR}, blocked PUB44-mediated CRCK3 ubiquitylation (Figure S4R). The data substantiate that CRCK3 is monoubiquitylated by PUB44 at multiple sites.

CRCK3 could be ubiquitylated *in vivo* using protoplasts co-expressing CRCK3-HA and FLAG-UBQ or FLAG-UBQ^{k0} (Figure 5C). To further examine whether PUB44 mediates CRCK3 ubiquitylation *in vivo*, we expressed HA-UBQ with PUB44-FLAG or PUB44^{C29A}-FLAG in protoplasts isolated from *p35S::gCRCK3-GFP*/WT transgenic plants. PUB44, but not PUB44^{C29A}, enhanced CRCK3 ubiquitylation (Figure 5D). PUB44 overexpression also increased the ubiquitylated CRCK3 proteins in *p35S::PUB44-HA*/*p35S::gCRCK3-GFP*/WT transgenic plants (Figure S5A). In addition, CRCK3 ubiquitylation was detected in *p35S::gCRCK3-GFP*/WT transgenic plants by immunoblotting with an α-UBQ antibody (Figure S5B). Furthermore, the *in vivo* ubiquitylated CRCK3 proteins obtained from transgenic plants or protoplasts could be eliminated upon incubation with GST-USP2-cc (Figures S5B and S5C). Consistently, the treatment of PYR-41, an E1 inhibitor, reduced PUB44-mediated CRCK3 ubiquitylation in *N. benthamiana* (Figure S5D). PYR-41 treatment also increased the protein abundance of CRCK3-GFP in *p35S::gCRCK3-GFP/p35S::PUB44-HA* transgenic plants (Figure S5E). Moreover, unlike PUB44, the inactive PUB44^{C29A} failed to reduce the CRCK3 protein abundance in *N. benthamiana* (Figure S5F). Meanwhile, the protein level of the CRCK3 ubiquitylation mutants, CRCK3^{7KR}, was not reduced by PUB44 while they were co-expressed in *N. benthamiana* (Figure S5G). Collectively, the data indicate that PUB44 ubiquitylates CRCK3, leading to CRCK3 degradation *in planta*.

PUB5 inhibits PUB44-mediated CRCK3 monoubiquitylation

A coIP assay using transgenic plants carrying *p35S::PUB44-HA*/*p35S::gPUB5-FLAG*/WT showed that PUB5-FLAG immunoprecipitated PUB44-HA *in vivo* (Figure 5E). PUB5 directly interacted with PUB44 *in vitro* (Figure S5H). Remarkably, HIS-PUB44-mediated CRCK3 monoubiquitylation was blocked by HIS-PUB5 in an *in vitro* ubiquitylation assay (Figure 5F). PUB10, which is an active E3 ligase,[29] did not ubiquitylate CRCK3 and did not affect PUB44-mediated CRCK3 monoubiquitylation (Figure S5I). Furthermore, the expression of PUB5-FLAG reduced PUB44-mediated ubiquitylation of CRCK3 in *p35S::gCRCK3-GFP*/WT transgenic plants (Figure 5G). Expression of the PUB5 ARM domain was sufficient to suppress PUB44-mediated CRCK3 ubiquitylation in *N. benthamiana* (Figure S5J), consistent with this domain interacting with CRCK3 (Figures 2D and S2C). Notably, the expression of PUB5 reduced the association of PUB44 with CRCK3, suggesting that PUB5 might compete with PUB44 for binding to CRCK3 (Figure S5K). The results collectively indicate that PUB5 acts to suppress the PUB44-mediated monoubiquitylation of CRCK3.

PUB5 inhibits the CRCK3 internalization, while PUB44 facilitates it

We observed vesicle-like internalized signals from CRCK3-GFP, which partially co-localized with red fluorescent protein (RFP)-tagged tandem repeat of the Fab1, YOTB, Vac1, and EEA1 (FYVE) domain (2xFYVE-RFP), an early endosome marker[35] in protoplasts (Figure S5L). In addition, CRCK3-GFP puncta co-localized with FM4-64, a lipophilic dye that labels the PM and is swiftly internalized by endocytosis,[36] in *p35S::gCRCK3-GFP*/WT transgenic plants (Figure S5M). The relative intracellular signals of CRCK3-GFP increased in *p35S::gCRCK3-GFP/pub5-1* compared with *p35S::gCRCK3-GFP*/WT (Figure 5H), suggesting that PUB5 suppresses CRCK3 internalization. Furthermore, transgenic plants expressing CRCK3-GFP in WT and *pub5-1* were treated with brefeldin A (BFA), a fungal toxin known to inhibit intracellular trafficking and induce protein internalization, forming BFA bodies in plant cells.[37] CRCK3-GFP signals in BFA bodies were markedly increased in *pub5-1* compared with WT (Figure 5I), further corroborating PUB5 suppressing CRCK3 internalization. In contrast, overexpression of PUB44, but not PUB13, increased the intracellularly internalized CRCK3-GFP signal intensity in *p35S::gCRCK3-GFP* transgenic plants, indicating that PUB44 promotes CRCK3-GFP internalization (Figure 5J). Notably, CRCK3 internalization was reduced upon PYR-41 treatment (Figure S5N), suggesting the ubiquitylation-dependent CRCK3-GFP internalization. Altogether, the data indicate that PUB5 and PUB44 exert opposite roles in regulating CRCK3 internalization, with PUB5 suppressing and PUB44 promoting it.

CRCK3 contributes to *Arabidopsis* defense against *Fusarium oxysporum*

Notably, *CRCK3* showed strong expression in root tips and root vasculatures of transgenic plants carrying *pCRCK3::GUS* or *pCRCK3::CRCK3-GFP* (Figure 6A). This prompted us to examine the responses of *crck3* mutants to the soil-borne root pathogen *F. oxysporum* f. sp. *conglutinans* strain 5176 (*Fo*5176). *Fo*5176 is known to colonize root xylem, depleting water and nutrients and causing wilting in *Arabidopsis*.[38] A *crck3* mutant allele, *summ3-17*, displayed significantly higher susceptibility to *Fo*5176 infection than WT (Figure 6B). Moreover, *pub5-1* also exhibited an increased susceptibility to *Fo*5176 infection (Figure 6B). *PUB5* is also expressed in root vasculatures (Figure S6A). The *CRCK3* expression under its native promoter in *summ3-17* recovered the susceptibility to *Fo*5176 infection to a similar level as WT (Figure 6C). These results support that CRCK3 is required for plant resistance against *Fo*5176 infections. Conversely, *Arabidopsis* plants overexpressing *CRCK3* under the *35S* promoter displayed less disease symptom development to *Fo*5176 than WT (Figure 6D). Additionally, we observed that CRCK3 protein levels increased in both leaves and roots of *p35S::gCRCK3-GFP*/WT transgenic plants upon *Fo*5176 infections (Figure 6E). Interestingly, SUMM2, which is expressed in shoots and roots (Figure S6B), did not play a significant role in resistance to *Fo*5176, as the susceptibility of *summ2-8* was comparable to WT (Figure S6C), suggesting that CRCK3/PUB5-mediated *F. oxysporum* resistance might operate independently of SUMM2.

To monitor the infection process of *Fo*5176 in plant roots, we introduced a GFP tag to *Fo*5176 and performed live-cell imaging using a confocal microscope in WT, *summ3-17*, and *p35S::gCRCK3-HA*/WT plants. Initially, *Fo*5176-GFP could colonize all three genotypes (Figure 6F). However, a notable distinction emerged as *Fo*5176-GFP hyphae exhibited a greater accumulation around root tips of *summ3-17* than WT and *p35S::gCRCK3-HA* plants. Furthermore, *Fo*5176-GFP exhibited accelerated and more extensive growth into the vascular tissues of *summ3-17* compared with its progression in WT and

Please cite this article in press as: Liu et al., The antagonistic role of an E3 ligase pair in regulating plant NLR-mediated autoimmunity and fungal pathogen resistance, Cell Host & Microbe (2024), https://doi.org/10.1016/j.chom.2024.06.004

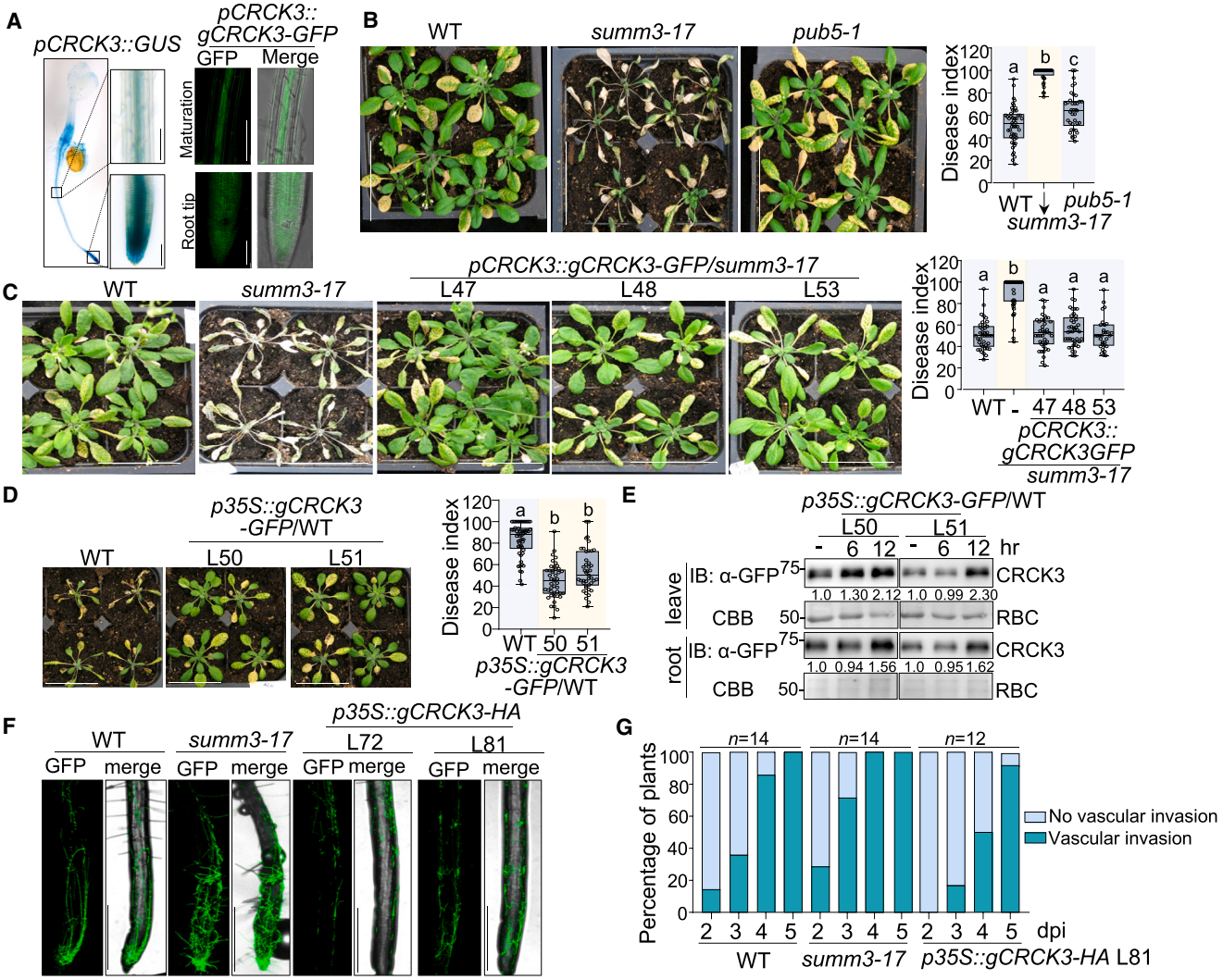

Figure 6. CRCK3 is involved in *Arabidopsis* response to *F. oxysporum*

(A) CRCK3 is expressed in root tissues. 4-day-old *pCRCK3::GUS* seedlings were stained with GUS. Scale bars: 100 μm (left). Confocal images of 4-day-old *pCRCK3::gCRCK3-GFP* transgenic seedlings are the result of a maximum projection generated from 10 images with a z-step of 1 μm, captured using a 63× lens. Scale bars: 100 μm (right).

(B) The *summ3-17* and *pub5-1* mutants are more susceptible to *Fo*5176 infections. Images were taken (left), and the disease index (right) was calculated 10 days post-infection (dpi) of *Fo*5176. Scale bars, 5 cm. Data are shown as box plots (n = 49 for WT, 40 for *summ3-17*, and 38 for *pub5-1*).

(C) CRCK3 complementation lines restore *summ3-17* susceptibility to *Fo*5176 to WT levels. The experiment and quantification were performed similarly as in (B) (n = 40 for WT, 48 for *summ3-17*, 41 for lines 47 and 48, and 31 for line 53). Scale bars, 5 cm.

(D) CRCK3 overexpression enhances *Arabidopsis* resistance against *Fo*5176. The images and quantification were taken at 13 dpi (n = 53 for WT, 45 for line 50, and 43 for line 51). Scale bars, 5 cm.

(E) CRCK3 protein levels were enhanced after *Fo*5176 infection. Roots of 1-week-old *p35S::gCRCK3-GFP* transgenic seedlings were infected with *Fo*5176. Numbers under the immunoblots indicate the relative densitometry of corresponding bands after normalizing to the control.

(F and G) CRCK3 regulates fungal invasion into vascular tissues. Roots of 6-day-old seedlings were treated with GFP-tagged *Fo*5176 for confocal imaging (F). Images represent a maximum projection of 44–50 images with a z-step of 5 μm using the 5× lens. Scale bars, 0.5 mm. The vascular tissue invasion rate (plants with vascular root tissues invaded by *Fo*5176 to total plants) is presented in (G). The number (n) of plants used for infection was labeled.

Experiments were repeated three times with similar results. Different letters in (B), (C), and (D) indicate a significant difference determined by one-way ANOVA followed by the Tukey test ($p < 0.05$).

See also Figure S6.

p35S::gCRCK3-HA plants (Figures 6F and 6G). This observation suggests that CRCK3 may play a pivotal role in impeding the invasion of fungal hyphae into vascular tissues, thereby contributing to the defense against *Fo*5176.

Cotton CRCK3 orthologs play an important role in plant defense against *F. oxysporum* infections

CRCK3 orthologs are present and highly conserved across a broad range of monocots and dicots, including economically

Please cite this article in press as: Liu et al., The antagonistic role of an E3 ligase pair in regulating plant NLR-mediated autoimmunity and fungal pathogen resistance, Cell Host & Microbe (2024), https://doi.org/10.1016/j.chom.2024.06.004

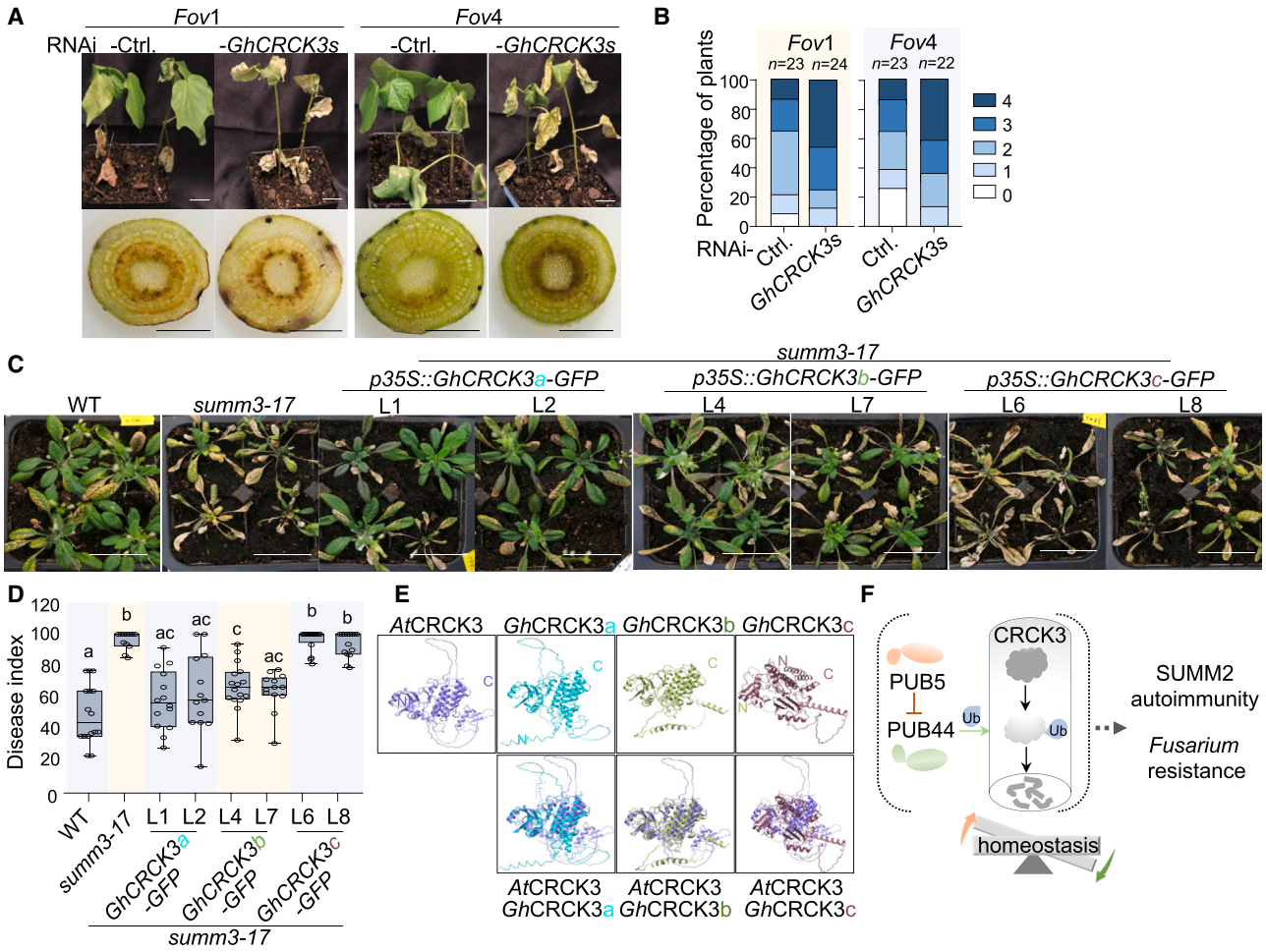

Figure 7. GhCRCK3a and GhCRCK3b, not GhCRCK3c, play a role in plant response to *F. oxysporum*

(A and B) Disease symptoms of leaves and stems in *Fov*-infected VIGS-*GhCRCK3s* and control plants. Images depicting the severity of foliar and plant wilting symptoms were taken at 12 dpi (A, top). Scale bars, 2 cm. The vascular discoloration was observed in the stem 1.5 cm above the soil line (A, bottom). Scale bars, 1 mm. The wilted leaves were counted at 10 dpi for disease ratings (B). The number (*n*) of plants used for each treatment is indicated.

(C and D) *GhCRCK3a* and *GhCRCK3b*, but not *GhCRCK3c*, rescue the *Fo*5176 resistance in *summ3-17*. Images were taken (C), and the disease index (D) was calculated at 10 dpi. Scale bars, 5 cm. Data are shown as box plots ($n = 16$ for WT, 12 for *summ3-17*, 14 for L1, 13 for L2, 16 for L4, 13 for L7, 16 for L6, 15 for L8). Scale bars, 5 cm. Different letters indicate a significant difference determined by one-way ANOVA followed by the Tukey test ($p < 0.05$).

(E) Predicted structure of *Arabidopsis* CRCK3 (*At*CRCK3) and its cotton homologs (*Gh*CRCK3). The structure was predicted using AlphaFold Protein Structure database (https://www.alphafold.ebi.ac.uk/). The overlay graph with their AlphaFold predicted structure was performed with ChimeraX software.

(F) A model of the CRCK3 proteostasis regulation by PUB5 and PUB44 in SUMM2-mediated autoimmunity and plant defense against *Fusarium*. PUB5 and PUB44 antagonistically regulate the CRCK3 proteostasis by controlling its monoubiquitylation, internalization, and degradation, subsequently regulating NLR SUMM2-mediated autoimmunity. The accumulation of CRCK3 is also crucial in mediating plant root immunity to prevent *Fusarium* infection by impeding its invasion into root vascular tissues.

Experiments were repeated three times with similar results.

See also Figures S6 and S7.

important crops that are highly susceptible to *F. oxysporum* infections, such as cotton (*Gossypium*) (Figure S6D). In the genome of allotetraploid upland cotton *G. hirsutum*, which accounts for a substantial portion of cotton production, three *CRCK3* homologs are identified. Each of these homologs is present in pairs in both "A" and "D" subgenomes, and they are denoted as *Gh*CRCK3a, *Gh*CRCK3b, and *Gh*CRCK3c, with the suffixes A or D indicating their cognate subgenomes (Figures S6E and S6F). Similar to *Arabidopsis* CRCK3, both *Gh*CRCK3a and *Gh*CRCK3c harbor an N-terminal signal peptide domain, a transmembrane (TM) domain, and a C-terminal kinase domain, whereas *Gh*CRCK3b lacks the TM domain (Figure S6E).

We deployed VIGS to simultaneously silence the expression of *GhCRCK3a*, *GhCRCK3b*, and *GhCRCK3c* in cotton (Figure S7A). Subsequently, we subjected these silenced plants to infections with two different races of *F. oxysporum f. sp. vasinfectum* (*Fov*), *Fov*1, and *Fov*4. Compared with VIGS vector control-inoculated plants, plants silenced *GhCRCK3s* showed more severe leaf wilting and a darker discoloration of vascular tissues in stems to both *Fov*1 and *Fov*4 infections (Figure 7A). Furthermore,

Please cite this article in press as: Liu et al., The antagonistic role of an E3 ligase pair in regulating plant NLR-mediated autoimmunity and fungal pathogen resistance, Cell Host & Microbe (2024), https://doi.org/10.1016/j.chom.2024.06.004

the quantification of the disease index, a measurement of the severity of disease symptoms, corroborated these findings (Figure 7B). These observations imply the crucial role of *Gh*CRCK3s in defending *Fov* infections in cotton.

To further investigate whether and which cotton *Gh*CRCK3s are functional orthologs of *Arabidopsis* CRCK3, we transformed individually the A-subgenome gene of *GhCRCK3a*, *GhCRCK3b*, or *GhCRCK3c* under the *35S* promoter into the *Arabidopsis summ3-17* mutant (Figure S7B). Transgenic plants carrying *p35S::GhCRCK3a* fully restored the resistance of *summ3-17* against *Fo*5176 to the WT level, while *p35S::GhCRCK3b* partially rescued resistance. On the other hand, *p35S::GhCRCK3c* failed to complement *summ3-17* susceptibility to *Fo*5176 (Figures 7C and 7D). Additionally, when examining cell death triggered by RNAi-*MEKK1* in *summ3-17*, *GhCRCK3a* and *GhCRCK3b*, but not *GhCRCK3c*, restored this response (Figure S7C). These data suggest that cotton *Gh*CRCK3a and *Gh*CRCK3b, but not *Gh*CRCK3c, are functional orthologs of *Arabidopsis* CRCK3, capable of conferring resistance to *F. oxysporum* and restoring the *mekk1*-mediated autoimmunity in *Arabidopsis*.

While all three *Gh*CRCK3s share a high degree of amino acid sequence conservation (Figure S7D), the AlphaFold2 prediction indicates that *Arabidopsis* CRCK3 shares a similar structure with *Gh*CRCK3a and *Gh*CRCK3b but not *Gh*CRCK3c (Figure 7E). Compared with *Gh*CRCK3a and *Gh*CRCK3b, *Gh*CRCK3c lacks two proline (P) residues before asparagine (N) at position 182 in the juxtamembrane (JM) domain (Figure S7E). When these two P residues were added to *Gh*CRCK3c, named *Gh*CRCK3c^{PP}, its structure became similar to that of *Gh*CRCK3b (Figures S7E and S7F), suggesting that the PP residues in the JM domain may be essential for stabilizing its overall structure.

DISCUSSION

In this study, we have unveiled a regulatory mechanism governing the proteostasis of the cytoplasmic kinase CRCK3, a pivotal player in SUMM2-mediated autoimmunity. CRCK3 protein levels are orchestrated by two closely related plant U-box E3 ligases, PUB5 and PUB44, operating in an antagonistic manner. PUB5 serves as a guardian of CRCK3 by counteracting the action of PUB44. Specifically, PUB5 thwarts PUB44-mediated monoubiquitylation and subsequent degradation of CRCK3, effectively leading to the stabilization of CRCK3 proteins (Figure 7F). Consequently, CRCK3 protein levels are substantially reduced in *pub5*, and overexpression of CRCK3 overcomes the defect of *pub5* in triggering SUMM2-mediated autoimmunity. Conversely, CRCK3 protein levels are increased in *pub44*, and the deletion of PUB44 leads to CRCK3-dependent autoimmunity. This result aligns with our earlier observation that elevated CRCK3 expression could induce cell death.[18] Thus, the protein abundance of CRCK3 is tightly controlled by PUB44-mediated degradation and PUB5-mediated stabilization.

Our study resembles a recent report about the antagonistic regulation of chloroplast-associated protein degradation by really interesting new gene (RING) domain UBQ E3 ligase suppressor of PPI1 locus 1 (SP1) and its homolog SP1-like 1 (SPL1).[39] Similar to PUB5, SPL1 lacks intrinsic E3 ligase activity. Yet, both SPL1 and PUB5 interfere with the ubiquitylation activity of their respective homologs, SP1 and PUB44.[39] Similarly, the human RING domain E3 ligase tripartite motif protein 67 (TRIM67) competes with its paralog TRIM9, inhibiting TRIM9-dependent ubiquitylation of the actin polymerase vasodilator-stimulated phosphoprotein (VASP).[40] In addition, TRIM26 non-catalytically inhibits the HECT-type E3 ligase WWP2 by competing for binding to the pluripotency transcription factor SOX2.[41] Hence, competition between different E3 ligases appears to be a common mechanism regulating E3 ligase activities in plants and metazoans.

Monoubiquitylation plays a crucial role in regulating various cellular processes, including protein trafficking, protein-protein interactions, DNA damage repair, transcriptional regulation, and endocytosis.[42] The E3 UBQ ligases RING-H2 FINGER A3A (RHA3A) and RHA3B monoubiquitylate RLCK BIK1 and regulate its dissociation from the PRR complex and endocytosis to initiate the downstream signaling.[34] RHA3A and RHA3B do not regulate BIK1 stability. Monoubiquitylation is also implicated in protein endocytosis and turnover. For example, monoubiquitylation of iron-regulated transporter 1 (IRT1) leads to its internalization/sorting and turnover, thereby keeping the PM pool of IRT1 low to ensure proper iron uptake and prevent metal toxicity.[43] *In vitro* and *in vivo* ubiquitylation assays indicate that CRCK3 is monoubiquitylated by PUB44. In addition, PUB44 promotes CRCK3-GFP internalization, suggesting that PUB44-mediated CRCK3 monoubiquitylation leads to its internalization. The most common mechanism by which internalized proteins are degraded is through the lysosomal/vacuolar degradation pathway.[44,45] Consistent with this view, CRCK3-GFP colocalizes with the early endosome marker and BFA bodies. The monoubiquitylated proteins could also be degraded by the UBQ-proteasome pathway in yeast and humans.[46] The observation that the treatment of proteasome inhibitor MG132 stabilizes CRCK3 supports this possibility.[18] Notably, monoubiquitylation- and polyubiquitylation-mediated protein degradation are interconnected. Monoubiquitylation could serve as a signal for subsequent polyubiquitylation events that could target proteins for degradation by the proteasome.[47]

The *pub44* mutant exhibits early senescence and autoimmunity-related seedling lethality that depends on TIR-type NLR (TNL) SOC3.[33,48,49] SUMM2 is a coiled-coil (CC)-type NLR (CNL). The autoimmunity of *pub44* is partially relieved in *summ2*, suggesting that the deletion of *PUB44* activates both TNL and CNL. Interestingly, overexpression of *PUB44* also triggers SOC3-dependent autoimmunity, signifying the abundance of PUB44 is essential for maintaining cellular homeostasis.[32,33] Here, we show that PUB44 ubiquitylates CRCK3 and reduces its protein abundance to avoid SUMM2-activated autoimmunity. Consistently, the *crck3* mutant partially suppresses the *pub44* autoimmunity. However, the targets of PUB44 in SOC3-mediated autoimmunity are still unknown. Although PUB44 associates with SOC3 in plants, they do not directly interact,[33] suggesting PUB44 might not ubiquitylate SOC3. Furthermore, the activation of SUMM2 and SOC3 in *pub44* is likely uncoupled since SUMM2-mediated *mekk1* cell death is independent of SOC3.

The RLCK family plays an essential role in plant defense against pathogen infections. In particular, RLCK VII subfamily members, such as BIK1, are key regulators of immune signaling initiated from PM-localized PRRs.[50,51] CRCK3 belongs to the RLCK IV subfamily, and their functions in plant disease

resistance are less characterized. CRCK3 is not required for bacterial MAMP flagellin-triggered PTI and effector AvrRpt2/AvrPphB-triggered ETI.[17] We show here that CRCK3 plays a conserved role in *Arabidopsis* and cotton defense against different races of *F. oxysporum*, suggesting CRCK3 might be involved in the signaling activated by a conserved component in *F. oxysporum*. Serval *F. oxysporum*-derived MAMPs, including chitin, serine-rich endogenous peptide (*Fo*SCOOP), and cell wall extract (*Fo*CWE), could trigger classical PTI responses and plant resistance to *F. oxysporum* infections.[52–55] It will be interesting to determine whether CRCK3 is involved in these MAMP-triggered immune responses. CRCK3 complexes with MLR LET2, which forms a trimeric complex with LET1 and LLG1.[19,22,23] Some MLRs and LLGs perceive plant endogenous rapid alkalinization factor (RALF) peptide ligands in orchestrating plant PTI and ETI.[56] MLR FERONIA (FER) negatively regulates plant immunity to *F. oxysporum* by perceiving *Fusarium*-derived RALF peptide.[57] LET-LLG1-CRCK3 cascade might coordinate with plant- and *Fusarium*-derived RALF peptides for an effective defense against *F. oxysporum*.

STAR★METHODS

Detailed methods are provided in the online version of this paper and include the following:

- KEY RESOURCES TABLE
- RESOURCE AVAILABILITY
  - Lead contact
  - Materials availability
  - Data and code availability
- EXPERIMENTAL MODEL AND STUDY PARTICIPANT DETAILS
  - *Arabidopsis thaliana* and growth conditions
  - *Nicotiana benthamiana* and growth conditions
  - Cotton and growth conditions
  - Fungal strains
- METHOD DETAILS
  - Positional cloning and next-generation sequencing
  - Plasmid construction and generation of transgenic plants
  - Agrobacterium-mediated virus-induced gene silencing (VIGS) assay
  - Transient expression assay in *Arabidopsis* protoplasts and *N. benthamiana*
  - RNA isolation and RT-PCR analysis
  - Trypan blue and DAB staining
  - Yeast two-hybrid assay
  - Co-IP assays
  - *In vivo* and *vitro* protein ubiquitylation assay
  - *In vitro* deubiquitylation assay
  - Split-luciferase assay
  - Recombinant protein isolation and *in vitro* pull-down assay
  - Confocal microscopy and FRET-FLIM assays
  - *Fusarium oxysporum* preparation, inoculation, and GFP transformation
  - Disease severity quantification and observation
  - Histochemical detection of β-Glucuronidase (GUS) activity
  - LC-MS/MS analysis
  - Phylogenetic tree analysis
  - Accession numbers
- QUANTIFICATION AND STATISTICAL ANALYSIS

SUPPLEMENTAL INFORMATION

Supplemental information can be found online at https://doi.org/10.1016/j.chom.2024.06.004.

ACKNOWLEDGMENTS

We thank the *Arabidopsis* Biological Resource Center (ABRC) for providing *Arabidopsis* T-DNA insertion lines, Dr. Mike Davis (University of California at Davis) for *Fov* isolates, and Dr. Lijun Ma (University of Massachusetts at Amherst) for *Fo*5176. The study was supported by the National Science Foundation (NSF) (IOS-2421016), USDA-NIFA (2023-67013-40858 and 2020-67013-41537), and the National Institutes of Health (NIH) (R35GM149197) to P.H.; NIH (R35GM144275) and NSF (IOS-2049642) to L.S.; and Fundamental Research Funds for the Central Universities, Sun Yat-sen University (24hytd011) to J.L.

AUTHOR CONTRIBUTIONS

J.L., Y.Y., P.H., and L.S. conceived the project, designed experiments, analyzed data, and wrote the manuscript with inputs from all authors. J.L. and Y.Y. identified PUB5, PUB44, and CRCK3; generated transgenic plants; and performed phenotype and interaction assays. J.L. performed ubiquitylation and disease assays. F.A.O.-M. performed microscopic assays. Y.Z., J.Z., and Y.C. contributed to ubiquitylation and interaction assays. D.L. contributed to internalization assays. Y.H. performed *pub5-1* mapping. L.K. contributed to protein structure prediction. Z.L. and M.Y. contributed to *Fusarium* resistance assays. D.G. contributed to protein purification. W.L. contributed to PUB5 cloning and mutant isolation. E.R. contributed to CRCK3 localization assays.

DECLARATION OF INTERESTS

The authors declare no competing interests.

Received: November 2, 2023
Revised: May 9, 2024
Accepted: June 4, 2024
Published: July 1, 2024

REFERENCES

1. Zhou, J.M., and Zhang, Y. (2020). Plant Immunity: Danger Perception and Signaling. Cell *181*, 978–989. https://doi.org/10.1016/j.cell.2020.04.028.
2. Jones, J.D.G., Staskawicz, B.J., and Dangl, J.L. (2024). The plant immune system: from discovery to deployment. Cell *187*, 2095–2116. https://doi.org/10.1016/j.cell.2024.03.045.
3. Couto, D., and Zipfel, C. (2016). Regulation of pattern recognition receptor signalling in plants. Nat. Rev. Immunol. *16*, 537–552. https://doi.org/10.1038/nri.2016.77.
4. Yu, X., Feng, B.M., He, P., and Shan, L.B. (2017). From Chaos to Harmony: Responses and Signaling upon Microbial Pattern Recognition. Annu. Rev. Phytopathol. *55*, 109–137. https://doi.org/10.1146/annurev-phyto-080516-035649.
5. Zhang, C., Xie, Y.P., He, P., and Shan, L.B. (2024). Unlocking Nature's Defense: Plant Pattern Recognition Receptors as Guardians Against Pathogenic Threats. Mol. Plant. Microbe Interact. *37*, 73–83. https://doi.org/10.1094/MPMI-10-23-0177-HH.
6. Cui, H., Tsuda, K., and Parker, J.E. (2015). Effector-triggered immunity: from pathogen perception to robust defense. Annu. Rev. Plant Biol. *66*, 487–511. https://doi.org/10.1146/annurev-arplant-050213-040012.
7. Sun, T.J., Nitta, Y., Zhang, Q., Wu, D., Tian, H.N., Lee, J.S., and Zhang, Y.L. (2018). Antagonistic interactions between two MAP kinase cascades in plant development and immune signaling. EMBO Rep. *19*, e45324. https://doi.org/10.15252/embr.201745324.
8. Bi, G.Z., Zhou, Z.Y., Wang, W.B., Li, L., Rao, S.F., Wu, Y., Zhang, X.J., Menke, F.L.H., Chen, S., and Zhou, J.M. (2018). Receptor-Like Cytoplasmic Kinases Directly Link Diverse Pattern Recognition Receptors to the Activation of Mitogen-Activated Protein Kinase Cascades in Arabidopsis. Plant Cell *30*, 1543–1561. https://doi.org/10.1105/tpc.17.00981.

9. Asai, T., Tena, G., Plotnikova, J., Willmann, M.R., Chiu, W.L., Gomez-Gomez, L., Boller, T., Ausubel, F.M., and Sheen, J. (2002). MAP kinase signalling cascade in innate immunity. Nature *415*, 977–983. https://doi.org/10.1038/415977a.

10. Gao, M.H., Liu, J.M., Bi, D.L., Zhang, Z.B., Cheng, F., Chen, S.F., and Zhang, Y.L. (2008). MEKK1, MKK1/MKK2 and MPK4 function together in a mitogen-activated protein kinase cascade to regulate innate immunity in plants. Cell Res. *18*, 1190–1198. https://doi.org/10.1038/cr.2008.300.

11. Ichimura, K., Casais, C., Peck, S.C., Shinozaki, K., and Shirasu, K. (2006). MEKK1 is required for MPK4 activation and regulates tissue-specific and temperature-dependent cell death in Arabidopsis. J. Biol. Chem. *281*, 36969–36976. https://doi.org/10.1074/jbc.M605319200.

12. Nakagami, H., Soukupová, H., Schikora, A., Zárský, V., and Hirt, H. (2006). A mitogen-activated protein kinase kinase kinase mediates reactive oxygen species homeostasis in Arabidopsis. J. Biol. Chem. *281*, 38697–38704. https://doi.org/10.1074/jbc.M605293200.

13. Petersen, M., Brodersen, P., Naested, H., Andreasson, E., Lindhart, U., Johansen, B., Nielsen, H.B., Lacy, M., Austin, M.J., Parker, J.E., et al. (2000). Arabidopsis MAP kinase 4 negatively regulates systemic acquired resistance. Cell *103*, 1111–1120. https://doi.org/10.1016/s0092-8674(00)00213-0.

14. Suarez-Rodriguez, M.C., Adams-Phillips, L., Liu, Y.D., Wang, H.C., Su, S.H., Jester, P.J., Zhang, S.Q., Bent, A.F., and Krysan, P.J. (2007). MEKK1 is required for flg22-induced MPK4 activation in Arabidopsis plants. Plant Physiol. *143*, 661–669. https://doi.org/10.1104/pp.106.091389.

15. Zhang, Z., Wu, Y., Gao, M., Zhang, J., Kong, Q., Liu, Y., Ba, H., Zhou, J., and Zhang, Y. (2012). Disruption of PAMP-induced MAP kinase cascade by a Pseudomonas syringae effector activates plant immunity mediated by the NB-LRR protein SUMM2. Cell Host Microbe *11*, 253–263. https://doi.org/10.1016/j.chom.2012.01.015.

16. Kong, Q., Qu, N., Gao, M., Zhang, Z., Ding, X., Yang, F., Li, Y., Dong, O.X., Chen, S., Li, X., and Zhang, Y. (2012). The MEKK1-MKK1/MKK2-MPK4 kinase cascade negatively regulates immunity mediated by a mitogen-activated protein kinase kinase kinase in Arabidopsis. Plant Cell *24*, 2225–2236. https://doi.org/10.1105/tpc.112.097253.

17. Zhang, Z., Liu, Y., Huang, H., Gao, M., Wu, D., Kong, Q., and Zhang, Y. (2017). The NLR protein SUMM2 senses the disruption of an immune signaling MAP kinase cascade via CRCK3. EMBO Rep. *18*, 292–302. https://doi.org/10.15252/embr.201642704.

18. Yang, Y., Liu, J., Yin, C., de Souza Vespoli, L., Ge, D., Huang, Y., Feng, B., Xu, G., Manhães, A.M.E.A., Dou, S., et al. (2020). RNA Interference-Based Screen Reveals Concerted Functions of MEKK2 and CRCK3 in Plant Cell Death Regulation. Plant Physiol. *183*, 331–344. https://doi.org/10.1104/pp.19.01555.

19. Liu, J., Huang, Y., Kong, L., Yu, X., Feng, B., Liu, D., Zhao, B., Mendes, G.C., Yuan, P., Ge, D., et al. (2020). The malectin-like receptor-like kinase LETUM1 modulates NLR protein SUMM2 activation via MEKK2 scaffolding. Nat. Plants *6*, 1106–1115. https://doi.org/10.1038/s41477-020-0748-6.

20. Nitta, Y., Qiu, Y., Yaghmaiean, H., Zhang, Q., Huang, J., Adams, K., and Zhang, Y. (2020). MEKK2 inhibits activation of MAP kinases in Arabidopsis. Plant J. *103*, 705–714. https://doi.org/10.1111/tpj.14763.

21. Su, S.H., Bush, S.M., Zaman, N., Stecker, K., Sussman, M.R., and Krysan, P. (2013). Deletion of a tandem gene family in Arabidopsis: increased MEKK2 abundance triggers autoimmunity when the MEKK1-MKK1/2-MPK4 signaling cascade is disrupted. Plant Cell *25*, 1895–1910. https://doi.org/10.1105/tpc.113.112102.

22. Huang, Y., Yin, C., Liu, J., Feng, B., Ge, D., Kong, L., Ortiz-Morea, F.A., Richter, J., Hauser, M.T., Wang, W.M., et al. (2020). A trimeric CrRLK1L-LLG1 complex genetically modulates SUMM2-mediated autoimmunity. Nat. Commun. *11*, 4859. https://doi.org/10.1038/s41467-020-18600-8.

23. Liu, Y., Zhong, X., Zhang, Z., Lan, J., Huang, X., Tian, H., Li, X., and Zhang, Y. (2021). Receptor-like kinases MDS1 and MDS2 promote SUMM2-mediated immunity. J. Integr. Plant Biol. *63*, 277–282. https://doi.org/10.1111/jipb.12978.

24. Takagi, M., Hamano, K., Takagi, H., Morimoto, T., Akimitsu, K., Terauchi, R., Shirasu, K., and Ichimura, K. (2019). Disruption of the MAMP-Induced MEKK1-MKK1/MKK2-MPK4 Pathway Activates the TNL Immune Receptor SMN1/RPS6. Plant Cell Physiol. *60*, 778–787. https://doi.org/10.1093/pcp/pcy243.

25. Takagi, M., Iwamoto, N., Kubo, Y., Morimoto, T., Takagi, H., Takahashi, F., Nishiuchi, T., Tanaka, K., Taji, T., Kaminaka, H., et al. (2020). Arabidopsis SMN7/HFN2, Encoding DEAD-Box RNA Helicase, Governs Proper Expression of the Resistance Gene SMN1/RPS6 and Is Involved in Dwarf, Autoimmune Phenotypes of mekk1 and mpk4 Mutants. Plant Cell Physiol. *61*, 1507–1516. https://doi.org/10.1093/pcp/pcaa071.

26. de Oliveira, M.V.V., Xu, G., Li, B., de Souza Vespoli, L., Meng, X., Chen, X., Yu, X., de Souza, S.A., Intorne, A.C., de A Manhães, A.M.E., et al. (2016). Specific control of Arabidopsis BAK1/SERK4-regulated cell death by protein glycosylation. Nat. Plants *2*, 15218. https://doi.org/10.1038/nplants.2015.218.

27. Mirdita, M., Schütze, K., Moriwaki, Y., Heo, L., Ovchinnikov, S., and Steinegger, M. (2022). ColabFold: making protein folding accessible to all. Nat. Methods *19*, 679–682. https://doi.org/10.1038/s41592-022-01488-1.

28. Trenner, J., Monaghan, J., Saeed, B., Quint, M., Shabek, N., and Trujillo, M. (2022). Evolution and Functions of Plant U-Box Proteins: From Protein Quality Control to Signaling. Annu. Rev. Plant Biol. *73*, 93–121. https://doi.org/10.1146/annurev-arplant-102720-012310.

29. Jung, C., Zhao, P., Seo, J.S., Mitsuda, N., Deng, S., and Chua, N.H. (2015). PLANT U-BOX PROTEIN10 Regulates MYC2 Stability in Arabidopsis. Plant Cell *27*, 2016–2031. https://doi.org/10.1105/tpc.15.00385.

30. Lu, D., Lin, W., Gao, X., Wu, S., Cheng, C., Avila, J., Heese, A., Devarenne, T.P., He, P., and Shan, L. (2011). Direct ubiquitination of pattern recognition receptor FLS2 attenuates plant innate immunity. Science *332*, 1439–1442. https://doi.org/10.1126/science.1204903.

31. Liang, W., van Wersch, S., Tong, M., and Li, X. (2019). TIR-NB-LRR immune receptor SOC3 pairs with truncated TIR-NB protein CHS1 or TN2 to monitor the homeostasis of E3 ligase SAUL1. New Phytol. *221*, 2054–2066. https://doi.org/10.1111/nph.15534.

32. Liang, W.W., Tong, M.X.Z., and Li, X. (2020). SUSA2 is an F-box protein required for autoimmunity mediated by paired NLRs SOC3-CHS1 and SOC3-TN2. Nat. Commun. *11*, 5190. https://doi.org/10.1038/s41467-020-19033-z.

33. Tong, M.X.Z., Kotur, T., Liang, W.W., Vogelmann, K., Kleine, T., Leister, D., Brieske, C., Yang, S.H., Lüdke, D., Wiermer, M., et al. (2017). E3 ligase SAUL1 serves as a positive regulator of PAMP-triggered immunity and its homeostasis is monitored by immune receptor SOC3. New Phytol. *215*, 1516–1532. https://doi.org/10.1111/nph.14678.

34. Ma, X., Claus, L.A.N., Leslie, M.E., Tao, K., Wu, Z., Liu, J., Yu, X., Li, B., Zhou, J., Savatin, D.V., et al. (2020). Ligand-induced monoubiquitination of BIK1 regulates plant immunity. Nature *581*, 199–203. https://doi.org/10.1038/s41586-020-2210-3.

35. Kutateladze, T.G. (2006). Phosphatidylinositol 3-phosphate recognition and membrane docking by the FYVE domain. Biochim. Biophys. Acta *1761*, 868–877. https://doi.org/10.1016/j.bbalip.2006.03.011.

36. Bolte, S., Talbot, C., Boutte, Y., Catrice, O., Read, N.D., and Satiat-Jeunemaitre, B. (2004). FM-dyes as experimental probes for dissecting vesicle trafficking in living plant cells. J. Microsc. *214*, 159–173. https://doi.org/10.1111/j.0022-2720.2004.01348.x.

37. Lam, S.K., Cai, Y., Tse, Y.C., Wang, J., Law, A.H.Y., Pimpl, P., Chan, H.Y.E., Xia, J., and Jiang, L.W. (2009). BFA-induced compartments from the Golgi apparatus and trans-Golgi network/early endosome are distinct in plant cells. Plant J. *60*, 865–881. https://doi.org/10.1111/j.1365-313X.2009.04007.x.

38. Wang, L., Calabria, J., Chen, H.W., Somssich, M., and Höfte, M. (2022). The Arabidopsis thaliana-Fusarium oxysporum strain 5176 pathosystem: an overview. J. Exp. Bot. *73*, 6052–6067. https://doi.org/10.1093/jxb/erac263.

39. Mohd Ali, S., Li, N., Soufi, Z., Yao, J., Johnson, E., Ling, Q., and Jarvis, R.P. (2023). Multiple ubiquitin E3 ligase genes antagonistically regulate chloroplast-associated protein degradation. Curr. Biol. *33*, 1138–1146.e5. https://doi.org/10.1016/j.cub.2023.01.060.

40. Boyer, N.P., McCormick, L.E., Menon, S., Urbina, F.L., and Gupton, S.L. (2020). A pair of E3 ubiquitin ligases compete to regulate filopodial dynamics and axon guidance. J. Cell Biol. *219*, e201902088. https://doi.org/10.1083/jcb.201902088.

41. Mahlokozera, T., Patel, B., Chen, H., Desouza, P., Qu, X., Mao, D.D., Hafez, D., Yang, W., Taiwo, R., Paturu, M., et al. (2021). Competitive binding of E3 ligases TRIM26 and WWP2 controls SOX2 in glioblastoma. Nat. Commun. *12*, 6321. https://doi.org/10.1038/s41467-021-26653-6.

42. Hicke, L. (2001). Protein regulation by monoubiquitin. Nat. Rev. Mol. Cell Biol. *2*, 195–201. https://doi.org/10.1038/35056583.

43. Barberon, M., Zelazny, E., Robert, S., Conéjéro, G., Curie, C., Friml, J., and Vert, G. (2011). Monoubiquitin-dependent endocytosis of the IRON-REGULATED TRANSPORTER 1 (IRT1) transporter controls iron uptake in plants. Proc. Natl. Acad. Sci. USA *108*, E450–E458. https://doi.org/10.1073/pnas.1100659108.

44. Li, F., Cheng, C., Cui, F., de Oliveira, M.V.V., Yu, X., Meng, X., Intorne, A.C., Babilonia, K., Li, M., Li, B., et al. (2014). Modulation of RNA polymerase II phosphorylation downstream of pathogen perception orchestrates plant immunity. Cell Host Microbe *16*, 748–758. https://doi.org/10.1016/j.chom.2014.10.018.

45. Mukhopadhyay, D., and Riezman, H. (2007). Proteasome-independent functions of ubiquitin in endocytosis and signaling. Science *315*, 201–205. https://doi.org/10.1126/science.1127085.

46. Braten, O., Livneh, I., Ziv, T., Admon, A., Kehat, I., Caspi, L.H., Gonen, H., Bercovich, B., Godzik, A., Jahandideh, S., et al. (2016). Numerous proteins with unique characteristics are degraded by the 26S proteasome following monoubiquitination. Proc. Natl. Acad. Sci. USA *113*, E4639–E4647. https://doi.org/10.1073/pnas.1608644113.

47. Skelly, M.J., Furniss, J.J., Grey, H., Wong, K.W., and Spoel, S.H. (2019). Dynamic ubiquitination determines transcriptional activity of the plant immune coactivator NPR1. eLife *8*, e47005. https://doi.org/10.7554/eLife.47005.

48. Vogelmann, K., Drechsel, G., Bergler, J., Subert, C., Philippar, K., Soll, J., Engelmann, J.C., Engelsdorf, T., Voll, L.M., and Hoth, S. (2012). Early senescence and cell death in Arabidopsis saul1 mutants involves the PAD4-dependent salicylic acid pathway. Plant Physiol. *159*, 1477–1487. https://doi.org/10.1104/pp.112.196220.

49. Raab, S., Drechsel, G., Zarepour, M., Hartung, W., Koshiba, T., Bittner, F., and Hoth, S. (2009). Identification of a novel E3 ubiquitin ligase that is required for suppression of premature senescence in Arabidopsis. Plant J. *59*, 39–51. https://doi.org/10.1111/j.1365-313X.2009.03846.x.

50. Liang, X., and Zhou, J.M. (2018). Receptor-Like Cytoplasmic Kinases: Central Players in Plant Receptor Kinase-Mediated Signaling. Annu. Rev. Plant Biol. *69*, 267–299. https://doi.org/10.1146/annurev-arplant-042817-040540.

51. Lin, W., Ma, X., Shan, L., and He, P. (2013). Big roles of small kinases: the complex functions of receptor-like cytoplasmic kinases in plant immunity and development. J. Integr. Plant Biol. *55*, 1188–1197. https://doi.org/10.1111/jipb.12071.

52. Hou, S., Liu, D., Huang, S., Luo, D., Liu, Z., Xiang, Q., Wang, P., Mu, R., Han, Z., Chen, S., et al. (2021). The Arabidopsis MIK2 receptor elicits immunity by sensing a conserved signature from phytocytokines and microbes. Nat. Commun. *12*, 5494. https://doi.org/10.1038/s41467-021-25580-w.

53. Rhodes, J., Yang, H.J., Moussu, S., Boutrot, F., Santiago, J., and Zipfel, C. (2021). Perception of a divergent family of phytocytokines by the Arabidopsis receptor kinase MIK2. Nat. Commun. *12*, 705. https://doi.org/10.1038/s41467-021-20932-y.

54. Babilonia, K., Wang, P., Liu, Z., Jamieson, P., Mormile, B., Rodrigues, O., Zhang, L., Lin, W., Danmaigona Clement, C., Menezes de Moura, S., et al. (2021). A nonproteinaceous Fusarium cell wall extract triggers receptor-like protein-dependent immune responses in Arabidopsis and cotton. New Phytol. *230*, 275–289. https://doi.org/10.1111/nph.17146.

55. Wang, P., Zhou, L., Jamieson, P., Zhang, L., Zhao, Z., Babilonia, K., Shao, W., Wu, L., Mustafa, R., Amin, I., et al. (2020). The Cotton Wall-Associated Kinase GhWAK7A Mediates Responses to Fungal Wilt Pathogens by Complexing with the Chitin Sensory Receptors. Plant Cell *32*, 3978–4001. https://doi.org/10.1105/tpc.19.00950.

56. Ortiz-Morea, F.A., Liu, J., Shan, L.B., and He, P. (2022). Malectin-like receptor kinases as protector deities in plant immunity. Nat. Plants *8*, 27–37. https://doi.org/10.1038/s41477-021-01028-3.

57. Masachis, S., Segorbe, D., Turrà, D., Leon-Ruiz, M., Fürst, U., El Ghalid, M., Leonard, G., López-Berges, M.S., Richards, T.A., Felix, G., and Di Pietro, A. (2016). A fungal pathogen secretes plant alkalinizing peptides to increase infection. Nat. Microbiol. *1*, 16043. https://doi.org/10.1038/nmicrobiol.2016.43.

58. Gao, X., Britt, R.C., Jr., Shan, L., and He, P. (2011). Agrobacterium-mediated virus-induced gene silencing assay in cotton. J. Vis. Exp. *54*, 2938. https://doi.org/10.3791/2938.

59. He, P., Shan, L., and Sheen, J. (2007). The use of protoplasts to study innate immune responses. Methods Mol. Biol. *354*, 1–9. https://doi.org/10.1385/1-59259-966-4:1.

60. Kong, L., Feng, B., Yan, Y., Zhang, C., Kim, J.H., Xu, L., Rack, J.G.M., Wang, Y., Jang, J.C., Ahel, I., et al. (2021). Noncanonical mono(ADP-ribosyl)ation of zinc finger SZF proteins counteracts ubiquitination for protein homeostasis in plant immunity. Mol. Cell *81*, 4591–4604.e8. https://doi.org/10.1016/j.molcel.2021.09.006.

61. Chen, H., Zou, Y., Shang, Y., Lin, H., Wang, Y., Cai, R., Tang, X., and Zhou, J.M. (2008). Firefly luciferase complementation imaging assay for protein-protein interactions in plants. Plant Physiol. *146*, 368–376. https://doi.org/10.1104/pp.107.111740.

62. Li, C., Guo, Y., Wang, L., and Yan, S. (2023). The SMC5/6 complex recruits the PAF1 complex to facilitate DNA double-strand break repair in Arabidopsis. EMBO J. *42*, e112756. https://doi.org/10.15252/embj.2022112756.

63. Zhou, X., Li, G., and Xu, J.R. (2011). Efficient approaches for generating GFP fusion and epitope-tagging constructs in filamentous fungi. Methods Mol. Biol. *722*, 199–212. https://doi.org/10.1007/978-1-61779-040-9_15.

64. Zhang, T., Hu, Y., Jiang, W., Fang, L., Guan, X., Chen, J., Zhang, J., Saski, C.A., Scheffler, B.E., Stelly, D.M., et al. (2015). Sequencing of allotetraploid cotton (Gossypium hirsutum L. acc. TM-1) provides a resource for fiber improvement. Nat. Biotechnol. *33*, 531–537. https://doi.org/10.1038/nbt.3207.

Please cite this article in press as: Liu et al., The antagonistic role of an E3 ligase pair in regulating plant NLR-mediated autoimmunity and fungal pathogen resistance, Cell Host & Microbe (2024), https://doi.org/10.1016/j.chom.2024.06.004

STAR★METHODS

KEY RESOURCES TABLE

REAGENT or RESOURCE	SOURCE	IDENTIFIER
Antibodies		
Rat anti-HA-Peroxidase	Roche	Cat#12013819001; RRID: AB_390917
Mouse anti-FLAG-Peroxidase	Sigma-Aldrich	Cat#A8592; RRID:AB_259529
Mouse anti-GFP	Roche	Cat#11814460001; RRID: AB_390913
Mouse anti-HIS-Peroxidase	Roche	Cat#11965085001; RRID: AB_514487
Mouse anti-GST-Peroxidase	Sigma-Aldrich	Cat#16-209; RRID: AB_310805
Rabbit anti-UBQ11	Agrisera	Cat#AS08 307; RRID: AB_2256904
Anti-mouse IgG HRP-linked antibody	Cell Signaling	Cat#7076; RRID: AB_330924
Anti-rabbit IgG HRP-linked antibody	Cell Signaling	Cat#7074; RRID: AB_2099233
Bacterial and fungal strains		
Agrobacterium tumefaciens GV3101	Liu et al.[19]	N/A
Escherichia coli BL21 (DE3)	Liu et al.[19]	N/A
Fusarium. oxysporum 5176 (*Fo*5176)	Wang et al.[55]	N/A
Fusarium. oxysporum f. sp vasinfectum 1 (*Fov1*)	Wang et al.[55]	N/A
Fusarium. oxysporum f. sp vasinfectum 4 (*Fov4*)	This paper	N/A
Chemicals, peptides, and recombinant proteins		
TRIzol™ Reagent	ThermoFisher	Cat#15596018
λ-phosphatase	New England Biolabs	Cat#P0753S
RNase-free DNase I	New England Biolabs	Cat#M0303L
IPTG	Sigma-Aldrich	Cat#I6758
Dexamethasone	Sigma-Aldrich	Cat#4902
Coomassie brilliant blue (CBB) R-250	ThermoFisher	Cat#20278
GelCode Blue Stain Reagent	ThermoFisher	Cat#24590
Ponceau S staining	Sigma-Aldrich	Cat#P7170
Protease Inhibitor Cocktail	Roche	Cat#12352200
Anti-FLAG M2 Affinity gel	Sigma-Aldrich	Cat#A2220
GFP-Trap agarose beads	Chromotek	Cat#gta-20
Pierce glutathione agarose	ThermoFisher	Cat#16101
Amylose resin	New England Biolabs	Cat#E8021L
HisPur™ Ni-NTA Resin	ThermoFisher	Cat#88222
ATP	Sigma-Aldrich	Cat#FLAAS
*At*UBQ	Bio-Techne	Cat #U-100At
UBQ	Bio-Techne	Cat #U-100H
UBQ^{k0}	Bio-Techne	Cat #UM-NOK
FM4-64	ThermoFisher	Cat #T13320
IPTG	Sigma-Aldrich	Cat# I6758
3,3'-Diaminobenzidine (DAB)	Sigma-Aldrich	Cat#D12384
Trypan blue	MP Biomedicals	Cat#195532
BFA	Sigma-Aldrich	Cat#B5936
PYR-41	MedChemExpress	Cat#HY-13296
Cycloheximide (CHX)	Sigma-Aldrich	Cat#239765
Critical commercial assays		
M-MuLV Reverse Transcriptase	New England Biolabs	Cat#M0253L
iTaq SYBR green Supermix	Bio-Rad	Cat#1725124

(*Continued on next page*)

Please cite this article in press as: Liu et al., The antagonistic role of an E3 ligase pair in regulating plant NLR-mediated autoimmunity and fungal pathogen resistance, Cell Host & Microbe (2024), https://doi.org/10.1016/j.chom.2024.06.004

Continued

REAGENT or RESOURCE	SOURCE	IDENTIFIER
ClonExpress II one Step Cloning Kit	Vazyme	Cat#C112-02
Bright-Glo™ Luciferase Assay	Promega	Cat#E2610
Experimental models: Organisms/strains		
Arabidopsis thaliana Col-0 wild-type	Liu et al.[19]	N/A
Arabidopsis thaliana Ler ecotype	Liu et al.[19]	N/A
Gossypium hirsutum 'CA 4002' (PI 665226)	Wang et al.[55]	N/A
pub5-1	ABRC	*salk_144599c*
pub5-2	ABRC	*gabi_003b11*
summ3-17	ABRC	*salk_039370*
pub44	ABRC	*salk_063974*
soc3-21	ABRC	*salk_200339*
summ2-8	ABRC	*salk_060294c*
pub44 summ3-17	This paper	N/A
pub44 summ2-8	This paper	N/A
AT3G28040	ABRC	*salk_053567*
AT3G28040	ABRC	*salk_093475*
mekk1	Liu et al.[19]	*salk_052557*
mpk4	Liu et al.[19]	N/A
mkk1 mkk2	Liu et al.[19]	N/A
mekk1 pub5-1	This paper	N/A
mpk4 pub5-1	This paper	N/A
mkk1 mkk2 pub5-1	This paper	N/A
pPUB5::gPUB5-GFP/pub5-1	This paper	N/A
p35S::gPUB5-FLAG/mekk1	This paper	N/A
p35S::gPUB5-FLAG/pub5-1	This paper	N/A
p35S::gPUB5^{C225A}-GFP/pub5-1	This paper	N/A
p35S::gPUB5^{W252A}-GFP/pub5-1	This paper	N/A
pPUB5::GUS/WT	This paper	N/A
p35S::MEKK2-HA/WT	This paper	N/A
p35S::MEKK2-HA/pub5-1	This paper	N/A
p35S::SUMM2^{ac}-HA/WT	This paper	N/A
p35S::SUMM2^{ac}-HA/pub5-1	This paper	N/A
pSUMM2::GUS/WT	This paper	N/A
pCRCK3::gCRCK3GFP/summ3-17	This paper	N/A
p35S::gCRCK3-GFP/WT	This paper	N/A
p35S::gCRCK3-GFP/pub5-1	This paper	N/A
p35S::gCRCK3-GFP/pub44	This paper	N/A
p35S::GhCRCK3a-GFP/summ3-17	This paper	N/A
p35S::GhCRCK3b-GFP/summ3-17	This paper	N/A
p35S::GhCRCK3c-GFP/summ3-17	This paper	N/A
pCRCK3::gCRCK3-GFP/pub5-1	This paper	N/A
pCRCK3::gCRCK3-GFP/pub44	This paper	N/A
p35S::gCRCK3-HA/WT	This paper	N/A
pCRCK3::GUS/WT	This paper	N/A
pCRCK3::gCRCK3-GFP/p35S::gPUB5-HA/pub5-1	This paper	N/A
p35S::gCRCK3-FLAG/p35S::PUB44-HA/WT	This paper	N/A
pCRCK3::gCRCK3-GFP/p35S::PUB44-HA/WT	This paper	N/A
pCRCK3::gCRCK3-GFP/p35S::PUB13-HA/WT	This paper	N/A
p35S::gPUB5-FLAG/p35S::PUB44-HA/WT	This paper	N/A

(*Continued on next page*)

Please cite this article in press as: Liu et al., The antagonistic role of an E3 ligase pair in regulating plant NLR-mediated autoimmunity and fungal pathogen resistance, Cell Host & Microbe (2024), https://doi.org/10.1016/j.chom.2024.06.004

Continued

REAGENT or RESOURCE	SOURCE	IDENTIFIER
Nicotiana benthamiana	Liu et al.[19]	N/A
Oligonucleotides		
Primers for cloning and point mutation, see Table S1	This paper	N/A
Primers for genotyping, see Table S1	This paper	N/A
Primers for RT-qPCR and VIGS, see Table S1	This paper	N/A
Recombinant DNA		
pHBT	Liu et al.[19]	N/A
pHBT-GFP-FLAG	This paper	N/A
pYL156 (pTRV-RNA2)	Yang et al.[18]	N/A
pTRV-RNA1	Yang et al.[18]	N/A
pYL156-CLA1	Yang et al.[18]	
pYL156-GFP	Yang et al.[18]	N/A
pYL156-BAK1/SERK4	Yang et al.[18]	N/A
pYL156-MEKK1	Yang et al.[18]	N/A
pYL156-GhCRCK3s	This paper	N/A
pYL156-PUB44	This paper	N/A
pHBT-FLAG-UBQ	Ma et al.[34]	N/A
pHBT-FLAG-UBQ^{k0}	Ma et al.[34]	N/A
pHBT-HA-UBQ	Liu et al.[19]	N/A
pHBT-PUB5-NLuc-HA	This paper	N/A
pHBT-PUB44-NLuc-HA	This paper	N/A
pHBT-CRCK3-Cluc-FLAG	This paper	N/A
pHBT-GFP-Cluc-FLAG	This paper	N/A
pHBT-CRCK3-FLAG	This paper	N/A
pHBT-PUB5-HA	This paper	N/A
pHBT-PUB5$^{U\text{-}box}$-HA	This paper	N/A
pHBT-PUB5^{ARM}-HA	This paper	N/A
pHBT-PUB5-GFP	This paper	N/A
pHBT-CRCK3-mCherry	This paper	N/A
pHBT-BIR2-mCherry	Liu et al.[19]	N/A
pHBT-BAK1-GFP	Liu et al.[19]	N/A
pHBT-PUB44-GFP	This paper	N/A
pHBT-PUB44-FLAG	This paper	N/A
pHBT-PUB44^{C29A}-FLAG	This paper	N/A
pHBT-PUB5-FLAG	This paper	N/A
pHBT-CRCK3-HA	This paper	N/A
pHBT-PUB44-HA	This paper	N/A
pHBT-PUB44^{C29A}-HA	This paper	N/A
pHBT-2XFYVE-RFP	This paper	N/A
pCB302-pPUB5::gPUB5-GFP	This paper	N/A
pCB302-p35S::gPUB5-FLAG	This paper	N/A
pCB302-p35S::gPUB5^{C225A}-GFP	This paper	N/A
pCB302-p35S::gPUB5^{W252A}-GFP	This paper	N/A
pCB302-p35S::gCRCK3-FLAG	This paper	N/A
pCB302-p35S::gCRCK3-GFP	Yang et al.[18]	N/A
pCB302-pCRCK3::gCRCK3-GFP	This paper	N/A
pCB302-pCRCK3::GUS	This paper	N/A
pCB302-pPUB5::GUS	This paper	N/A

(*Continued on next page*)

Please cite this article in press as: Liu et al., The antagonistic role of an E3 ligase pair in regulating plant NLR-mediated autoimmunity and fungal pathogen resistance, Cell Host & Microbe (2024), https://doi.org/10.1016/j.chom.2024.06.004

Continued

REAGENT or RESOURCE	SOURCE	IDENTIFIER
pCB302-pSUMM2::GUS	This paper	N/A
pCB302-p35S::GhCRCK3a-GFP	This paper	N/A
pCB302-p35S::GhCRCK3b-GFP	This paper	N/A
pCB302-p35S::GhCRCK3c-GFP	This paper	N/A
pCB302-p35S::LET1-GFP	This paper	N/A
pCAMBIA2300-p35S::gCRCK3-HA	This paper	N/A
pCAMBIA2300-p35S::CRCK3^{7KR}-GFP	This paper	N/A
pCAMBIA2300-p35S::PUB5-FLAG	This paper	N/A
pCAMBIA2300-p35S::PUB5$^{U\text{-}box}$-FLAG	This paper	N/A
pCAMBIA2300-p35S::PUB5^{ARM}-FLAG	This paper	N/A
pCAMBIA2300-p35S::PUB5^{IF1}-FLAG	This paper	N/A
pCAMBIA2300-p35S::PUB5$^{IF1\ 3}$-FLAG	This paper	N/A
pCAMBIA2300-p35S::PUB5$^{IF1\ 2\ 3}$-FLAG	This paper	N/A
pCAMBIA2300-p35S::PUB5$^{IF2\ 3}$-FLAG	This paper	N/A
pCAMBIA2300-p35S::PUB5^{IF2}-FLAG	This paper	N/A
pCAMBIA2300-p35S::PUB5^{IF3}-FLAG	This paper	N/A
pCAMBIA2300-p35S::PUB44-FLAG	This paper	N/A
pCAMBIA2300-p35S::PUB44^{C29A}-FLAG	This paper	N/A
pCAMBIA2300-p35S::FLAG-UBQ	This paper	N/A
pCAMBIA2300-p35S::PUB44-GFP	This paper	N/A
pMDC-2xp35S::PUB44-HA	This paper	N/A
pMDC-2xp35S::gPUB5-HA	This paper	N/A
pMDC-2xp35S::MEKK2-HA	Liu et al.[19]	N/A
pMDC-2xp35S::SUMM2ac-HA	Liu et al.[19]	N/A
pMDC-2xp35S::PUB13-HA	Lu et al.[30]	N/A
pMDC-2xp35S::MEKK2-GFP	Liu et al.[19]	N/A
pMDC-2xp35S::SUMM2-GFP	Liu et al.[19]	N/A
pET28a-PUB5	This paper	N/A
pET28a-PUB44	This paper	N/A
pET28a- PUB44^{C29A}	This paper	N/A
pET28a-PUB13	Lu et al.[30]	N/A
pET22b-AtUBA1	Ma et al.[34]	N/A
pET22b-AtUBC8	Ma et al.[34]	N/A
pGST-USP2-cc	Ma et al.[34]	N/A
pGST-CRCK3^{CD}	This paper	N/A
pGST	Liu et al.[19]	N/A
pMAL-PUB5	This paper	N/A
pMAL-PUB10	This paper	N/A
pMAL	Liu et al.[19]	N/A
pCB302	Liu et al.[19]	N/A
pGBKT7-PUB5	This paper	N/A
pGADT7-CRCK3	This paper	N/A
pGADT7	Ma et al.[34]	N/A
pGBKT7	Ma et al.[34]	N/A
Software and algorithms		
ImageJ	NIH	RRID:SCR_003070; https://imagej.nih.gov/ij/

(*Continued on next page*)

Please cite this article in press as: Liu et al., The antagonistic role of an E3 ligase pair in regulating plant NLR-mediated autoimmunity and fungal pathogen resistance, Cell Host & Microbe (2024), https://doi.org/10.1016/j.chom.2024.06.004

Continued

REAGENT or RESOURCE	SOURCE	IDENTIFIER
Proteome discoverer 2.5	ThermoFisher	N/A
Leica Application Suite X (LAS X) software	Leica	Version 3.5.5.19976; RRID:SCR_013673
GraphPad Prism 9	GraphPad	RRID: SCR_002798
ChimeraX 1.6.1	UCSF	RRID:SCR_015872; https://www.cgl.ucsf.edu/chimerax/
LTQ Orbitrap XL LC-MS/MS system	Thermo Scientific	N/A
Mascot	Matrix Science	Version 2.2.2 RRID:SCR_014322
MEGA11	MEGA	RRID:SCR_023017

RESOURCE AVAILABILITY

Lead contact

Further information and requests for resources and reagents should be directed to and will be fulfilled by the lead contact, Ping He (pinghemi@umich.edu).

Materials availability

Plasmids and transgenic plants generated in this study will be made available upon request to the scientific community, but we may require a payment and/or a completed Materials Transfer Agreement.

Data and code availability

- The published article includes all datasets generated or analyzed during this study. All data are publicly available as of the date of publication. Sequence data from this article were retrieved in TAIR (https://www.arabidopsis.org/, accession code: PRJNA10719) for *Arabidopsis* and in CottonGen database (http://www.cottongen.org) with the Nanjing Agricultural University (NAU) assembly (accession code: PRJNA248163) for *G. hirsutum*.
- This paper does not report the original code.
- Any additional information required to reanalyze the data reported in this paper is available from the lead contact upon request.

EXPERIMENTAL MODEL AND STUDY PARTICIPANT DETAILS

Arabidopsis thaliana and growth conditions

Arabidopsis accession Col-0 (WT), mutants, and transgenic plants used in this study were grown in soil (LP5 RSi, Sun Gro Horticulture, USA) or ½ MS medium in a growth room at 23°C, 45-55% humility, and 75 μE m^{-2} s^{-1} light with a 12-hr light/ 12-hr dark photoperiod. The *pub5-1* (*salk_144599c*), *pub5-2* (*gabi_003b11*), *summ3-17* (*salk_039370*), *pub44* (*salk_063974*), *soc3-21* (*salk_200339*), *summ2-8* (*salk_060294c*), *salk_053567*, and *salk_093475* mutant lines were obtained from Arabidopsis Biological Resource Center (ABRC). The mutants of *mekk1*, *mkk1 mkk2*, *mpk4*, and *summ2-8* were reported previously.[19,22] The *pub44 summ3-17* and *pub44 summ2-8* double mutants were generated by crossing with the corresponding single mutants. Seedlings were grown on plates containing half-strength Murashige and Skoog medium (½MS) with 0.5% sucrose, 0.8% agar, and 2.5 mM MES at pH 5.7 in a growth room with the same condition as the above.

Nicotiana benthamiana and growth conditions

Nicotiana benthamiana was grown in a growth room in soil under a 12-hr light/12-hr dark photoperiod at 23°C.

Cotton and growth conditions

G. hirsutum 'CA 4002' (PI 665226) was grown in 3.5-inch square pots containing PRO-LINEC/25 soil (JollyGardener, USA) at 23°C, 30% humidity, and 150 μ$Em^{-2}s^{-1}$ light with a 12-hr light/12-hr dark photoperiod. Two-week-old cotton plants were used for *Agrobacterium*-mediated virus-induced gene silencing (VIGS) assays.[55]

Fungal strains

The Fungal strains used in this study were described in the key resources table. *Fusarium oxysporum Fo*5176, *F. oxysporum f. sp vasinfectum* (*Fov*) race 1 (*Fov*1) isolate CA10, and race 4 isolate CA14 (*Fov4*) were grown on potato dextrose agar plates (PDA, 200 g potato, 20 g glucose, 20 g agar, and 1 L water) at 23°C. For spores separation, the hyphae of *Fov* and *Fo*5176 were inoculated in YEPD medium (10 g yeast extract, 20 g peptone, 20 g glucose for 1 L) and incubated in a shaker (120 g) at 23°C.

Please cite this article in press as: Liu et al., The antagonistic role of an E3 ligase pair in regulating plant NLR-mediated autoimmunity and fungal pathogen resistance, Cell Host & Microbe (2024), https://doi.org/10.1016/j.chom.2024.06.004

METHOD DETAILS

Positional cloning and next-generation sequencing

The *let3* mutant was crossed to the heterozygous *mekk1* mutant to obtain the *let3*/*mekk1* double homozygous mutant, which suppressed the *mekk1* seedling lethality but still showed growth defects distinguishable from WT plants. The *let3*/*mekk1* mutant in the Col-0 background was crossed to the ecotype Landsberg *erecta* (L*er*-0). Two pools of plants, including 30 WT-looking plants and 30 *let3*/*mekk1*-looking plants from the F_2 population, were selected for genomic DNA isolation and PCR-based mapping analysis. The genetic mapping, next-generation sequencing (NGS), and data analyses followed a previous report.[44] Briefly, 22 pairs of simple sequence length polymorphism (SSLP) markers evenly distributed on five chromosomes of *Arabidopsis* were used to screen the length polymorphisms between two mixed DNA pools consisting of an equal amount of DNAs from 30 individual plants in each pool. The initial mapping placed both *LET3* and *MEKK1* (*AT4G08500*) on chromosome 4 based on the bulked segregation analysis. Additional SSLP markers from chromosome 4 with 205 *let3*/*mekk1*-looking plants from the F_2 population further mapped *LET3* between markers of *M4E13* and *F20D10*. We then performed NGS of *let3* with 100-nucleotide paired-end sequencing on an Illumina HiSeq2000 platform at Texas AgriLife Genomics and Bioinformatics Service (TAGS). Forty-fold genome coverage was obtained. Illumina reads were mapped to the TAIR10 release of the Col-0 genome using CLC Genomics Workbench 6.0.1 software (http://www.clcbio.com). The candidate variants between *M4E13* and *F20D10* were selected, and an 818-bp fragment deletion was found in the *AT4G36550* gene, which encodes plant U-box protein 5 (PUB5). The mutation was further confirmed with Sanger sequencing using genomic DNA.

Plasmid construction and generation of transgenic plants

The coding sequences (CDS) or genomic DNA regions of *PUB5* and *CRCK3* were amplified from genomic DNA or cDNA of *Arabidopsis* wild-type Col-0. The CDS or genomic DNA fragment of *PUB5* (*gPUB5*) or *CRCK3* (*gCRCK3*) was inserted into *pHBT-p35S::FLAG*, *pHBT-p35S::HA, pHBT-p35S::GFP, pCB302-p35S::FLAG, pCB302-p35S::GFP, pCAMBIA2300-p35S::FLAG*, or *pCAMBIA2300-p35S::HA* vector using a one-step cloning kit (Vazyme, China) by BamHI and StuI digestion. To generate the site-directed mutagenesis of protein variants, site mutations were introduced into primers, and the fragments were linked by a one-step cloning kit (Vazyme, China). To generate *pCB302-pCRCK3::gCRCK3-GFP* and *pCB302-pCRCK3::GUS*, the 2,000-bp genomic DNA fragment upstream of the *CRCK3* start codon was amplified from WT *Arabidopsis* genomic DNA and replaced the *35S* promotor of *pCB302-p35S::gCRCK3-GFP* or *pCB302-p35S::GUS* by SacI and BamHI digestion. To generate *pCB302-pPUB5::gPUB5-GFP* and *pCB302-pPUB5::GUS*, the 2,052-bp genomic DNA fragment upstream of the *PUB5* start codon was amplified from *Arabidopsis* genomic DNA and replaced the *35S* promotor of *pCB302-p35S::gPUB5-GFP* or *pCB302-p35S::GUS* with SacI and BamHI digestion. To generate *pCB302-pSUMM2::GUS*, the 2,000-bp genomic DNA fragment upstream of the *SUMM2* start codon was amplified from *Arabidopsis* genomic DNA and replaced the *35S* promotor of *pCB302-p35S::GUS* with SacI and BamHI digestion. To generate *pMDC32-p35S::PUB44-HA* and *pMDC32-p35S::PUB13-HA* constructs, the coding sequence of each gene was amplified from cDNA of *Arabidopsis* Col-0 and cloned into a modified *pMDC32-p35S::HA* vector with BamHI and StuI digestion. *pHBT-p35S::HA-UBQ*, *pHBT-p35S::FLAG-UBQ, pMDC32-p35S::MEKK2-HA*, and *pMDC32-35S::SUMM2^{ac}-HA* constructs were described previously.[19,22,34] To generate *pCAMBIA2300-p35S::FLAG-UBQ*, the FLAG-UBQ fragment with stop codon after *UBQ* was amplified from *pHBT-p35S::FLAG-UBQ*, and cloned into *pCAMBIA2300-p35S::FLAG* vector with BamHI and StuI digestion.

The *PUB5* or *CRCK3* coding sequence fragment was inserted into the modified *pGBKT7* or *pGADT7* vector with BamHI and StuI digestion for the yeast two-hybrid assay. The coding sequence of *PUB5*, *PUB44*, *PUB13*, or *CRCK3* cytoplasmic domain (CD) was inserted into the *pET28a* vector with BamHI and HindIII digestion for protein expression in *E. coli* BL21. To generate *pGSTu-CRCK3^{CD},* the fragment of CRCK3^{CD} was amplified by PCR and cloned into a modified Glutathione S-transferase (GST) fusion protein expression vector *pGSTu* with BamHI and StuI digestion. To generate *pET28-HIS-PUB5, pET28-HIS-PUB44*, and *pET28-HIS-PUB13* constructs, the CDS fragments of *PUB5*, *PUB44*, and *PUB13* were amplified by PCR and cloned into a modified HIS fusion protein expression vector *pET28* with BamHI and HindIII digestion. To generate *pMAL-PUB5* and *pMAL-PUB10*, the fragments of *PUB5* and *PUB10* CDS were amplified by PCR and cloned into MBP fusion protein expression vector *pMAL* with BamHI and StuI digestion. To generate *pHBT-p35S::gCRCK3-Cluc-FLAG* and *pHBT-p35S::GFP-Cluc-FLAG*, the fragments of *CRCK3* and *GFP* were amplified from the *pHBT* vector and subcloned into *pHBT-p35S::Cluc-FLAG* by BamHI and SpeI digestion using a one-step cloning kit. To generate *pHBT-p35S::gPUB5-Nluc-HA* and *pHBT-p35S::PUB44-Nluc-HA*, *PUB44* or *PUB5* sequence was cloned into *pHBT-p35S::Nluc-HA* using a one-step cloning kit by BamHI and SpeI digestion.

The coding sequences of *GhCRCK3s* were cloned from the cDNA of *G. hirsutum*, and inserted into *pCB302* binary vector using a one-step cloning kit by BamHI and StuI digestion to generate *pCB302-p35S::GhCRCK3s-GFP* constructs. To generate the *VIGS-GhCRCK3s* construct, fragments corresponding to *GhCRCK3a* (300-bp), *GhCRCK3b* (300-bp), and *GhCRCK3c* (300-bp) were amplified from the cotton cDNA library and inserted into *pYL156* (*pTRV-RNA2*) vector with EcoRI and KpnI digestion. To generate the *VIGS-PUB44*, fragments corresponding to *PUB44* (300-bp) were amplified from *Arabidopsis* cDNA library and inserted into *pYL156* (*pTRV-RNA2*) vector with EcoRI and KpnI digestion.

Primer sequences were listed in Table S1, and all insertions in different vectors were verified by Sanger sequencing.

Transgenic plants were generated using *Agrobacterium tumefaciens*-mediated floral dipping. Transgenic plants were screened by glufosinate-ammonium (Basta, 50 μg/ml) for the *pCB302* vector, hygromycin (50 μg/ml) for *pCAMBIA1300* and *pMDC32*, and confirmed by immunoblotting for protein expression.

Please cite this article in press as: Liu et al., The antagonistic role of an E3 ligase pair in regulating plant NLR-mediated autoimmunity and fungal pathogen resistance, Cell Host & Microbe (2024), https://doi.org/10.1016/j.chom.2024.06.004

Agrobacterium-mediated virus-induced gene silencing (VIGS) assay

The *Agrobacterium tumefaciens* strain GV3101 harboring *pYL156-RNA1*, *pYL156-MEKK1*, *pYL156-BAK1/SERK4*, *pYL156-GhCRCK3s, pYL156-PUB44, pYL156-CLA1*, or *pYL156-GFP* (the vector control) was grown overnight in LB medium with 50 μg/ml kanamycin, 50 μg/ml gentamycin, 10 mM MES, and 20 μM acetosyringone. The cells were pelleted by 3,500 rpm centrifugation at room temperature for 10 min, resuspended in infiltration solution (10 mM MES, 10 mM $MgCl_2$, and 200 μM acetosyringone), and incubated at room temperature for 3 hr. Cultures containing the *pYL156-MEKK1*, *pYL156-BAK1/SERK4*, *pYL156-GhCRCK3s, pYL156-PUB44, pYL156-CLA1*, or *pYL156-GFP* were mixed with *pYL156-RNA1* cultures at 1:1 ratio, individually. For *Arabidopsis* infiltration, the mixed cultures were inoculated into the first pair of true leaves of 10-day-old *Arabidopsis* seedlings using a needleless syringe. The albino phenotype (*VIGS-CLA1*) or cell death phenotype (*VIGS-MEKK1*) usually shows two weeks post infiltration. For cotton, the mixed cultures were inoculated into the pair of cotyledons of two-week-old seedlings using a needleless syringe.[58]

Transient expression assay in *Arabidopsis* protoplasts and *N. benthamiana*

The indicated *pHBT* constructs were used for protoplast transfection following the protocol. Briefly, for co-IP assay, 100 μl of plasmid DNA (2 μg/μl) was mixed with 1 ml of protoplasts (2 x 10^5 cells/ml), and for split-luciferase assay, 50 μl of plasmid DNA (2 μg/μl) was mixed with 500 μl cells, for the PEG-mediated transfection.[59] For transient assays in *N. benthamiana*, the indicated constructs were transferred into *A. tumefaciens* strain GV3101 by electroporation. A single transformant was transferred into 2 ml LB liquid medium containing 50 μg /ml kanamycin and 25 μg/ml gentamicin for overnight incubation at 28°C. Bacteria were harvested by centrifugation at 1,200 g and resuspended in the buffer of 10 mM $MgCl_2$ at OD_{600}=1. The *Agrobacterial* cultures were infiltrated into the leaves of four-week-old *N. benthamiana*. Proteins were isolated 2-3 days after inoculation from the infiltrated area and subjected to immunoblotting analysis.

RNA isolation and RT-PCR analysis

Total RNAs were prepared using the TRIzol reagent (Invitrogen, USA). The RNase-free DNase I (New England Biolabs, USA) was used to remove contaminating genomic DNA. Complementary DNAs (cDNAs) were synthesized with M-MuLV Reverse Transcriptase (New England Biolabs, USA) and oligo(dT) primers. Quantitative RT-PCR analysis was performed using iTaq Universal SYBR green Supermix (Bio-Rad, USA) with a CFX384™ Real-Time system (Bio-Rad, USA). RT-PCR analysis was performed with gene-specific primers, and PCR products were analyzed by agarose gel electrophoresis. The expression of each gene was normalized to the expression of *UBQ10* for qRT-PCR and *UBQ1* or *GhUBI1* for RT-PCR.

Trypan blue and DAB staining

Detached leaves were soaked in trypan blue staining solution (2.5 mg/ml trypan blue dissolved in lactophenol containing an equal volume of lactic acid, glycerol, liquid phenol, and ddH_2O) or 3, 3'-diaminobenzidine (DAB) solution (1 mg/ml DAB dissolved in ddH_2O, pH 3.8) for overnight incubation. Samples were transferred into trypan blue destaining solution containing lactophenol and ethanol in a ratio of 1:2 or DAB destaining solution containing glycerol, acetic acid, and ethanol in a ratio of 1:1:3 and incubated at room temperature with gentle shaking until entirely destained. Samples were observed and recorded under a dissecting microscope.

Yeast two-hybrid assay

The cDNA library in the *pGADT7* vector used for yeast two-hybrid screen was described previously.[60] About 110,000 colonies were screened for interaction with the PUB5 in *pGBKT7* (Clontech, USA) in the synthetic defined (SD) medium without histidine, leucine, and tryptophan (SD-H-L-T) and supplemented with 1 mM 3-amino-1, 2, 4-triazole (3-AT). The positive clones were further confirmed with targeted yeast two-hybrid assays, and the gene identity was revealed by sequencing and BLAST search.

Co-IP assays

Proteins were expressed overnight in *Arabidopsis* protoplasts, or isolated from the transgenic lines. Protoplasts were lysed by vertexing, and leaves were grounded in the extraction buffer (100 mM NaCl, 1 mM EDTA, 20 mM Tris-HCl, pH 7.5, 2 mM NaF, 2 mM Na_3VO_4, 1 mM DTT, 0.5% Triton X-100, 10% glycerol, and 1 x protease inhibitor). After centrifugation at 12,500 g at 4°C for 15 min, 250 μl extraction buffer was added to dissolve pellets, 20 μl supernatant was collected for input controls, and the remaining was incubated with α-FLAG affinity beads (Sigma, USA) or α-GFP-trap agarose beads (Chromotek, Germany) at 4°C for 1 hr with gentle shaking. Beads were collected and washed three times with washing buffer (20 mM Tris-HCl, pH 7.5, 100 mM NaCl, 1 mM EDTA, 0.5% Triton X-100), and once with 50 mM Tris-HCl, pH 7.5. Proteins were eluted by 2 × SDS-PAGE loading buffer and boiled at 94°C for 5 min. Immunoprecipitated and input proteins were analyzed by immunoblotting with indicated antibodies. For co-IP assay with samples from transgenic plants, total proteins were extracted from 2 g leaves of four-week-old plants with 2 ml IP buffer (100 mM NaCl, 1 mM EDTA, 20 mM Tris-HCl, pH 7.5, 0.5% Triton X-100, 10% glycerol). The supernatant was collected after centrifugation at 10,000 g for 10 min at 4°C, followed by another centrifugation at 12,500 g for 30 min at 4°C. The FLAG-tagged proteins and the associated proteins were purified from the cell lysates with α-FLAG affinity beads by immunoprecipitation. The beads were boiled with 2 × SDS-PAGE loading buffer at 94°C for 5 min to elute the proteins. Immunoprecipitated and input proteins were analyzed by immunoblotting with indicated antibodies.

Please cite this article in press as: Liu et al., The antagonistic role of an E3 ligase pair in regulating plant NLR-mediated autoimmunity and fungal pathogen resistance, Cell Host & Microbe (2024), https://doi.org/10.1016/j.chom.2024.06.004

In vivo and *vitro* protein ubiquitylation assay

For *in vivo* ubiquitylation assay, FLAG-tagged genes (40 μg DNA) were co-expressed with HA-UBQ or vector control (40 μg DNA) in 1-ml protoplasts at the density of 2 x 10^5/ml for 12 hr, or HA-UBQ or vector control was expressed in the protoplasts from *p35S::gCRCK3-GFP* transgenic plants. In *N. benthamiana*, CRCK3-HA was co-expressed with FLAG-UBQ or control vector via *Agrobacterial*-mediated transient expression for 60 hr. Proteins were collected as the above-mentioned co-IP assay in an IP buffer containing 0.5% Triton X-100. The *in vitro* ubiquitylation assay was performed as previously.[34] Briefly, reactions containing 1 μg substrate, 1 μg HIS-E1 (AtUBA1), 1 μg HIS-E2 (AtUBC8) or human E2 (UBC13/UEV1A) (Boston Biochem, USA), 1 μg GST-E3, 1 μg human UBQ, or human UBQ with no lysine (K) mutant (UBQ^{K0}), or FLAG-tagged human UBQ (FLAG-UBQ) (Boston Biochem, USA) in the 30 μl of the ubiquitylation reaction buffer (20 mM Tris-HCl, pH 7.5, 5 mM $MgCl_2$, 0.5 mM DTT, 2 mM ATP) were incubated at 24°C for 8 hr. The ubiquitylated proteins were detected by immunoblotting with indicated antibodies.

In vitro deubiquitylation assay

The deubiquitylating enzyme (DUB) of mouse GST-USP2-cc was used for the deubiquitylation assay as described previously.[34] In brief, an *in vitro* ubiquitylation assay was performed at 24°C for 8 hr, as described above, in 60 μl of the ubiquitylation reaction buffer. The reaction was aliquoted into two individual tubes (30 μl for each) with or without 1 μg GST-USP2-cc at 28°C for 1 hr. Samples were then denatured and analyzed by immunoblotting. To obtain *in vivo* ubiquitylated CRCK3 proteins, CRCK3-FLAG and HA-UBQ were expressed in *Arabidopsis* protoplasts. The ubiquitylated CRCK3-FLAG proteins were immunoprecipitated with α-FLAG affinity beads; CRCK3-GFP was immunoprecipitated from 2 g of four-week-old *p35S::gCRCK3-GFP*/WT transgenic plants with GFP-trap agarose beads (Chromotek, Germany). The beads were mixed with 1 μg GST-USP2-cc in 50 μl of DUB reaction buffer (25 mM Tris-HCl, pH 7.5, 150 mM NaCl, and 10 mM DTT) at 28°C for 1 hr. The beads were denatured in the SDS-PAGE loading buffer and analyzed by immunoblotting.

Split-luciferase assay

The Cluc-FLAG and Nluc-HA tagged proteins were co-expressed in protoplasts for 12 hr.[61] The cells were lysed by extraction buffer (100 mM NaCl, 1 mM EDTA, 20 mM Tris-HCl, pH 7.5, 2 mM NaF, 2 mM Na_3VO_4, 1 mM DTT, 0.5% Triton X-100, 10% glycerol, and 1 x protease inhibitor). The cell lysis was centrifuged at 12,500 g at 4°C for 15 min. 10 μl of supernatant was mixed with 30 μl of H_2O and 10 μl of 1 mM luciferin in a cell of the 96-well plate. The reaction mixture was incubated at room temperature for 5 min. The luminescence was measured using a luminometer (Promega GloMax Navigator, USA).

Recombinant protein isolation and *in vitro* pull-down assay

Fusion proteins were produced from *E. coli* BL21 at 16°C using LB medium with 0.25 mM isopropyl-β-d-thiogalactoside (IPTG). Glutathione S-transferase (GST) fusion proteins were purified with Pierce glutathione agarose (Thermo Scientific, USA), HIS fusion proteins were purified using Ni-NTA agarose (Qiagen, USA), and Maltose-binding protein (MBP) fusion proteins were purified using amylose resin (NEB lab, USA) according to the standard protocol from companies. HIS-tagged PUB5 and PUB44 proteins were incubated with GST or GST-$CRCK3^{CD}$ in the pull-down buffer (20 mM Tris-HCl, pH 7.5, 100 mM NaCl, 0.1 mM EDTA, 0.2% Triton X-100) for 1 hr with gentle shaking, subsequently incubated with 20 μl of glutathione agarose at 4°C for another 2 hr with gentle shaking. Beads were washed five times with pull-down buffer (20 mM Tris-HCl, pH 7.5, 100 mM NaCl, 0.1 mM EDTA, 0.2% Triton X-100), and boiled in 50 μl of 2 x SDS protein loading buffer for 10 min and detected by immunoblotting with an α-HIS antibody. The amylose resin was used for the MBP fusion protein pull-down assay, as previously described.[62]

Confocal microscopy and FRET-FLIM assays

The GFP and mCherry fusion proteins were detected using a Leica TCS SP8 confocal laser scanning microscope (Germany). The GFP was excited at 488 nm, and emission was detected between 490 and 530 nm. The mCherry fluorescence was excited at 587 nm, and emission was detected between 590 and 620 nm. The RFP fluorescence was excited at 547 nm, and emission was detected between 581 and 647 nm. For the FM 4-64 staining, the excitation/emission was 515/640 nm, respectively. To measure fluorescence signal intensity, confocal images were converted to 8-bit in ImageJ. Regions of interest (ROIs) were selected based on plasma membrane (PM) or cytosol localization. Histograms listing all intensity values per ROI were generated, and the averages of the top 10% most intense pixels were used for the calculation of relative PM/intracellular fluorescence intensity. To analyze CRCK3-GFP internalization, five-day-old *Arabidopsis* seedlings grown on ½MS were imaged with a 63 x oil-corrected immersion objective lens (numerical aperture of 1.40) on an inverted confocal laser scanning microscope (Leica TCS SP8, Germany). The excitation/emission wavelengths used were 488 nm/490-530 nm, respectively. The pinhole was set at 1 Airy unit. Images were captured using Leica Application Suite X (LAS X) software.

For the FRET-FLIM assay, the pinhole was set at 1 Airy unit. Images and FLIM/FRET analyses were performed by using Leica Application Suite X (LAS X) software as described. Briefly, FRET measurements were done with a pair of GFP/mCherry fusion proteins. The image of GFP donor fluorescence was analyzed and scanned at 488 nm and detected between 490 and 530 nm. The fluorescence lifetime (τ) was calculated as the average of 20 τ values randomly measured in the protoplast cells. The values obtained for 20 protoplasts were used to determine the average value of τ for each pair of proteins analyzed. The relative fluorescence intensity (I) in a certain region of interest (ROI), lifetime (τ), and FRET efficiency were measured by the Leica LAS X software. FRET efficiency (E) was calculated by using the formula E = 1-(τDA/τD). τDA is the lifetime of the donor in the presence of the acceptor, and τD is the

Please cite this article in press as: Liu et al., The antagonistic role of an E3 ligase pair in regulating plant NLR-mediated autoimmunity and fungal pathogen resistance, Cell Host & Microbe (2024), https://doi.org/10.1016/j.chom.2024.06.004

fluorescence lifetime of the donor alone. The statistical analysis was performed by one-way ANOVA for multiple comparisons, and asterisks indicated significant differences ($p < 0.01$).

Fusarium oxysporum preparation, inoculation, and GFP transformation

*Fusarium oxysporum Fo*5176, *F. oxysporum f. sp vasinfectum* (*Fov*) race 1 (*Fov*1) isolate CA10, and race 4 isolate CA14 (*Fov4*) were grown on potato dextrose agar plates (Difco) for four days at room temperature (23°C). The hyphae of *Fov* and *Fo*5176 were inoculated in YEPD medium (10 g yeast extract, 20 g peptone, 20 g glucose for 1 L) and incubated in a shaker (120 g) at room temperature (23°C) for three days. The spores were collected from the medium by filtering through Miracloth (Millipore). After centrifugation at 4,000 g for 15 min, the spores were resuspended with sterile water and adjusted to the final concentration. The inoculum of 1×10^7 spores/ml was used for *Fov* and *Fo*5176 inoculation with the root-dipping method for *Arabidopsis* and cotton.[54,55] Briefly, three-week-old *Arabidopsis* or cotton plants two weeks after VIGS were gently uprooted from the soil, and the roots were briefly washed with water to remove big chunks of dirt. After removing excess water with paper towels, the roots were immersed in *Fo*5176 or *Fov* spore suspension for 3 min and then planted in pots with pre-wet soil. After inoculation, plants were covered with a dome to hold 90% humidity and kept at 23°C and 75 $\mu E\ m^{-2}\ s^{-1}$ light with a 12-hr light/12-hr dark photoperiod for three days. The plants were transferred into a growth chamber at 28°C, 50% humidity, and 100 $\mu E\ m^{-2}\ s^{-1}$ light with a 12-hr light/12-hr dark photoperiod. For *Fo*5176 infection assay of *Arabidopsis* in plates, the seeds were germinated on ½MS plates for two days at room temperature and then transferred to a 28°C chamber for another six days. The roots were incubated with 3 ml H_2O or *Fo*5176 spores (1×10^7/ml) for 2 min, and the extra liquid was removed. The seedlings were kept in the 28°C chambers for 6 or 12 hr, and the roots and leaves were harvested to detect CRCK3-GFP proteins. The seedlings were grown in the 28°C chamber for another six days to record the infection phenotype.

To make GFP-tagged *Fo*5176, *Fo*5176 protoplasts were transformed with a broad-host vector *pDL2-GFP*, in which the GFP gene with a mutation at phenylalanine 64 to leucine for enhanced GFP signals (EGFP) is under the control of the *Magnaporthe oryzae* ribosomal protein 27 (*RP27*) promoter.[63] *F. oxysporum* protoplast isolation and transformation followed the previous publication.[52] The transformants were examined by fluorescence microscope and immunoblotting using an α-GFP antibody. The transformants bear no detectable difference from the wild-type *Fo*5176 strain in terms of morphology, pigmentations, and pathogenicity.

Disease severity quantification and observation

The disease index was calculated as previously described.[55] The disease index for *Arabidopsis* is presented as the percentage of the leaves showing chlorosis or wilting to the total leaves of the inoculated plants. For VIGSed cotton plants, the severity of the disease symptoms on each cotton seedling was scored using a 0 to 4 rating scale, where 0 = no visible chlorosis or wilting symptoms; 1 = one true leaf with chlorosis or wilting symptoms; 2 = two true leaves wilted or dropped off; 3 = more than two true leaves wilted or dropped off; and 4 = the whole plant wilted, or all leaves dropped off. To observe stem discoloration, thin sections of the stem, approximately 1.5 cm above the soil line, were collected and analyzed using the Olympus SZX10 stereomicroscope.

Histochemical detection of β-Glucuronidase (GUS) activity

Four-day-old plate-growth *Arabidopsis* seedlings were immersed and vacuumed in the GUS staining solution [10 mM EDTA, 1% Tween 10, 2 mM $K_3Fe(CN)_6$, 2 mM $K_4Fe(CN)_6$, and 2 mM X-Gluc in 50 mM PBS, pH 7.0] for 30 min, followed by incubation at 37 °C for 2-12 hr. Samples were cleared in chloral hydrate for 6 hr, followed by photographing using the Olympus SZX10 stereomicroscope.

LC-MS/MS analysis

For CRCK3-associated protein identification, CRCK3-GFP was transiently expressed in 30 ml of protoplasts (2×10^5 cells/ml) for 12 hr. The cells were lysed in the IP buffer by vertexing and followed by centrifugation at 12,500 g for 15 min at 4°C. The supernatant was incubated with GFP-trap magnetic agarose (ChromoTek, Germany) for 1 hr at 4°C with gentle shaking on a rocker. The beads were collected and washed five times with washing buffer, and the CRCK3 complexes were eluted with elution buffer (60 μl of 0.5% SDS, 25 mM Tris, pH 7.5). The sample was digested by trypsin to generate the peptides for liquid chromatography-tandem mass spectrometry (LC-MS/MS) analysis at UT Southwestern Medical Center. The MS/MS spectrum was analyzed using MaxQuant software with the default parameters. The identified peptides were searched against the *Arabidopsis* protein database (TAIR11) to obtain detailed protein information. For CRCK3 ubiquitylation site identification, the PUB44-mediated CRCK3 ubiquitylation was performed *in vitro*, and samples were sent for LC-MS/MS analysis at the Biological Mass Spectrometry Facility at the University of Michigan, as previously described.[34]

Phylogenetic tree analysis

Protein sequences were obtained from the *Arabidopsis* Information Resource (TAIR) and NCBI databases, and *Gh*CRCK3 protein sequences were obtained from the databases of Nanjing Agricultural University (NAU) assembly for *G. hirsutum*.[64] ClustalW was used to generate multiple sequence alignments. For constructing phylogenetic trees, the neighbor-joining method with 1,000 bootstrap replicates was applied using MEGAX in the program MEGA X. The resulting trees were viewed on an interactive tree of life (iTOL, https://itol.embl.de/).

Please cite this article in press as: Liu et al., The antagonistic role of an E3 ligase pair in regulating plant NLR-mediated autoimmunity and fungal pathogen resistance, Cell Host & Microbe (2024), https://doi.org/10.1016/j.chom.2024.06.004

Accession numbers

Sequence data from this article were retrieved in TAIR (https://www.arabidopsis.org/, accession code: PRJNA10719) for *Arabidopsis* and in CottonGen database (http://www.cottongen.org) with the Nanjing Agricultural University (NAU) assembly (accession code: PRJNA248163) for *G. hirsutum* under the following accession numbers: *PUB5* (*AT4G36550*), *CRCK3* (*AT2G11520*), *PUB44* (*AT1G20780*), *PUB13* (*AT3G46510*), *PUB10* (*AT1G71020*), *MEKK1* (*AT4G08500*), *MKK1* (*AT4G26070*), *MKK2* (*AT4G29810*), *MEKK2* (*AT4G08480*), *SUMM2* (*AT1G12280*), *MPK4* (*AT4G01370*), *PR1* (*AT2G14610*), *PR2* (*AT3G57260*), *UBQ10* (*AT4G05320*), *CRCK1* (*AT5G58940*), *CRCK2* (*AT4G00330*), *GhUBI1* (*Gh_A12G1442*), *GhCRCK3aA* (*Gh_A06G0453*), *GhCRCK3aD* (*Gh_D06G0493*), *GhCRCK3bA* (*Gh_A08G2104*), *GhCRCK3bD* (*Gh_D08G2474*), *GhCRCK3cA* (*Gh_A05G0070*), and *GhCRCK3cD* (*Gh_D05G0128*), *GhCRCK1A* (*Gh_A07G0932*), *GhCRCK1D* (*Gh_D07G1010*), *GhCRCK2aA* (*Gh_A07G1304*), *GhCRCK2aD* (*Gh_D07G1415*), *GhCRCK2bA* (*Gh_A11G0814*), *GhCRCK2bD* (*Gh_D11G0955*).

QUANTIFICATION AND STATISTICAL ANALYSIS

Data for quantification analyses are presented as mean ± standard error (SEM) or standard deviation (SD), or box plots. Box plots show the first and third quartiles, split by the medians (lines), with whiskers extending a 1.5-fold interquartile range beyond the box. The statistical analyses were performed with the Student's *t*-test or one-way analysis of variance (ANOVA) test (* $P < 0.05$, ** $P < 0.01$, *** $P < 0.001$). The number of replicates is shown in the figure legends. Microsoft Excel 2016 and Graphpad Prism 8 (Graphpad Prism software, version 8.0.1) were used for statistics, and bar graphs were overlaid with dot plots.